

A comparative study of *Cocconeis scutellum* Ehrenberg and its varieties (Bacillariophyta)

Mario De Stefano^{1,*}, Oscar E. Romero²
and Cecilia Totti³

¹ Department of Environmental Science, the Second University of Naples, Via Vivaldi 43, 81100 Caserta, Italy, e-mail: mario.destefano@unina2.it

² Instituto Andaluz de Ciencias de la Tierra (IACT-CSIC), Facultad de Ciencias, Universidad de Granada, Campus Fuentenueva, 18002 Granada, Spain

³ Department of Marine Sciences, Università Politecnica delle Marche, Via Brecce Bianche, 60131 Ancona, Italy

* Corresponding author

Abstract

We present an ultrastructure-based revision (using light and electron microscopy) of the type species of the genus *Cocconeis*, *C. scutellum* var. *scutellum*, and four often-mentioned but poorly described, morphologically related varieties: *C. scutellum* var. *baldjikiana*, *C. scutellum* var. *clinoraphis*, *C. scutellum* var. *parva*, *C. scutellum* var. *posidoniae*. In addition, we introduce three new taxa, *C. scutellum* var. *gorensis* var. nov., *C. scutellum* var. *posidoniae* f. *decussata* f. nov. and *C. scutellum* var. *sullivanensis* var. nov. The taxonomic relationships between these varieties and the remaining validly described *C. scutellum* varieties are analyzed on the basis of their ultrastructural differences. We also provide additional information on the geographical distribution of all analyzed *C. scutellum* taxa.

Keywords: biogeography; *Cocconeis scutellum*; electron microscopy; ultrastructure.

Introduction

The monoraphid genus *Cocconeis* Ehrenberg ranks among the most architecturally complex diatom genera because of its heterovalvarity, elaborate, and functionally complex girdle bands and intricately ornamented valves (e.g., Kobayasi and Nagumo 1985, Round et al. 1990, De Stefano and De Stefano 2005, De Stefano and Romero 2005). The genus *Cocconeis* is known to be benthic, with the raphe-sternum valves firmly attached to rocks, plants, animals, or any other substrata, where they may constitute communities with high specimen abundance and species richness (Sullivan 1979, 1981, 1982, Romagnoli et al. 2006, Totti et al. 2007). VanLandingham (1968, 1979) recorded 314 valid taxa of *Cocconeis*, with the majority described solely on the examination of only one valve, usually the sternum or rapheless valve, which is more strongly silicified and easily dislodged from the

substratum (Romero and Navarro 1999, De Stefano and Romero 2005).

Within the genus *Cocconeis*, *C. scutellum* Ehrenberg is the most commonly reported species in ecological and taxonomic studies, with more than 100 reports focusing solely on this species and its infraspecific taxa (Gaul et al. 1993). However, the *C. scutellum* complex still remains poorly studied in terms of valvar architecture and distinctive taxonomic features, which have caused considerable confusion in past and current taxonomic and ecological reports (Hustedt 1959, Romero 1996, De Stefano et al. 2000). *C. scutellum* is the type species for the genus (Ehrenberg 1838) and was lectotypified by Boyer (1927). Its valvar morphology is simple and can be easily distinguished in light microscopy (Romero 1996, De Stefano 2001, De Stefano and Romero 2005). The main diagnostic features of *C. scutellum* are monolayered valves with uniseriate striae covering most of the valve face, becoming bi- or triseriate on the mantle, and circular poroids occluded by hymenes with radially arranged linear perforations (Mann 1981, Romero 1996, De Stefano and De Stefano 2005, De Stefano and Romero 2005). A total of 14 validly described taxa are reported by VanLandingham (1968, 1979).

Here, we provide an ultrastructure-based revision of four poorly described varieties of *Cocconeis scutellum*, viz. var. *baldjikiana* (Grunow) Cleve, var. *clinoraphis* Zanon, var. *parva* Grunow, var. *posidoniae* De Stefano, Marino et Mazzella, and we propose two varieties (var. *gorensis* and var. *sullivanensis*) and one form new to science (var. *posidoniae* f. *decussata*). The diagnostic valve features of the *C. scutellum* taxa studied here were compared with those of the type species and of the remaining valid varieties (VanLandingham 1968, 1979) in so far as these are available from the literature. Our comparative study on *C. scutellum* varieties shows that the ultrastructural differences of both valves, rather than morphometric data, allow reliable identification for most of these taxa. The possibility of identifying four main lineages within *C. scutellum* varieties based on ultrastructural differences was also explored.

Materials and methods

Samples containing taxa of the *Cocconeis scutellum* complex collected from *Posidonia* leaves, and historical collection and sampling locations are listed in Table 1. Leaf samples of *P. oceanica* (Linnaeus) Delile were collected in the spring of 2005 and 2006 (the season of low densities of epiphytic macroalgae) covering as much as possible the Mediterranean basin (Table 1), and leaf samples of *P. coriacea* Cambridge et Kuo and *P. sinuosa* Cambridge et Kuo were also collected during the austral spring of 2003 and 2004 off Rottneest Island, Western

Table 1 List of diatom taxa in the *Cocconeis scutellum* complex examined from historical collection and current material collected from leaves of *Posidonia* species in the Mediterranean Sea and Western Australia.

Diatom taxon	Source of material	Locality
<i>Cocconeis scutellum</i> var. <i>scutellum</i>	<i>Posidonia oceanica</i>	Western to eastern Mediterranean Sea Italy: Genoa, east and west Sardinia, Ventotene and Ischia islands, Pizzo Calabro, Milazzo, Otranto, Taranto Spain: Medas Island, Alicante, Majorca Macedonia: Delimara Slovenia: Izola Croatia: Split Greece: Saronico Gulf, Patmos Island Turkey: Edremit and Kusadasi Gulfs
<i>Cocconeis scutellum</i> var. <i>baldjikiana</i>	Slide E74 Hustedt diatom collection <i>Posidonia oceanica</i>	Italy: Lissa-Rovigno Southern Tyrrhenian, Adriatic and Aegean Seas Italy: Pizzo Calabro, Milazzo, Otranto, Taranto Slovenia: Izola
<i>Cocconeis scutellum</i> var. <i>clinoraphis</i>	<i>Posidonia sinuosa</i>	Rottneest Island, Western Australia Nancy Cove, Philip Rock
<i>Cocconeis scutellum</i> var. <i>gorensis</i>	<i>Posidonia coriacea</i>	Rottneest Island, Western Australia Nancy Cove, Philip Rock
<i>Cocconeis scutellum</i> var. <i>parva</i>	<i>Posidonia oceanica</i>	Western to eastern Mediterranean Sea Italy: Genoa, Ventotene Island Spain: Majorca Macedonia: Delimara Greece: Patmos Island Turkey: Edremit and Kusadasi Gulfs
<i>Cocconeis scutellum</i> var. <i>posidoniae</i>	<i>Posidonia oceanica</i>	Western to eastern Mediterranean Sea Italy: Genoa, east and west Sardinia, Ventotene and Ischia islands, Pizzo Calabro, Milazzo, Otranto, Taranto Spain: Medas Island, Alicante, Majorca Macedonia: Delimara Slovenia: Izola Croatia: Split Greece: Saronico Gulf, Patmos Island Turkey: Edremit and Kusadasi Gulfs
<i>Cocconeis scutellum</i> var. <i>posidoniae</i> f. <i>decussata</i>	<i>Posidonia oceanica</i>	Southern Adriatic Sea Italy: Otranto Slovenia: Izola Croatia: Split
<i>Cocconeis scutellum</i> var. <i>sullivanensis</i>	<i>Posidonia oceanica</i>	Southern Tyrrhenian Sea Italy: Ventotene and Ischia islands

Australia. In each locality, 40 *Posidonia* shoots were sampled at a depth of 5 m by SCUBA divers who cut leaves from the rhizomes at the level of the ligulae; leaves were placed on a Plexiglas board. The epiphytic microalgae were removed from both leaf surfaces by scraping with a scalpel and rinsed in a Petri dish with distilled or filtered seawater (0.2 µm pore size Nuclepore® filter, Nuclepore, Pleasanton, CA, USA). The collected material was transferred to a tube with a final volume of 20–30 ml of concentrated scraped material. Part of the samples was fixed with 4% neutralized formaldehyde for microscopic observation, and the remainder was treated to remove the organic matter. The diatom material was cleaned with 70% nitric acid at 60°C for 1 h, washed several times

with distilled water, then treated with concentrated sulphuric acid, washed again and used to prepare permanent slides with Hyrax® (Penn & Ruedrich, Ass., CA Eastern agent: Eimer & Amend, New York, USA). Slides were examined with a Zeiss Axiophot light microscope (LM) (Carl Zeiss, Oberkochen, Germany). Cleaned material was also mounted on stubs and sputter-coated with gold or platinum for scanning electron microscopy (SEM) (Jeol 6060, Jeol Ltd., Tokyo, Japan), or mounted on formvar-coated grids for transmission electron microscopy (TEM) (Philips 400, Philips Electron Optics BV, Eindhoven, The Netherlands).

The terminology follows Anonymous (1975), Ross et al. (1979), Holmes et al. (1982) and Round et al. (1990), while

the classification follows Round et al. (1990). The stria density was usually counted near the apical axis center but also at the opposite margin to the center if the striae were markedly radiate.

Results (Figures 1–152)

Order Achnanthes Silva

Family Cocconeidaceae Kützing

Genus *Cocconeis* Ehrenberg

Cocconeis scutellum Ehrenberg var. *scutellum* (Figures 19–35)

Basionym *Cocconeis scutellum* Ehrenberg 1838, p. 194, pl. 14, fig. 8.

Synonyms *Cocconeis mediterranea* Kützing 1844, p. 73, pl. 5, fig. VI-8. *Cocconeis peruviana* Kützing 1844, p. 73, pl. 5, fig. VI-7. *Cocconeis brundusiaca* Rabenhorst 1853, p. 28, pl. 3, fig. 16. *Cocconeis ambigua* Grunow 1867–1870, p. 14, pl. 1, fig. 9. *Cocconeis scutellum* var. *gemmata* (Ehrenberg) Schmidt 1894 in Schmidt et al. 1874–1959, pl. 190, figs. 23, 24. *Cocconeis scutellum* var. *dilatata* Schmidt 1894 in Schmidt et al. 1874–1959, pl. 190, figs. 25, 26. *Cocconeis scutellum* var. *morrisii* (W. Smith) Peragallo et Peragallo 1897–1908, p. 19, pl. 1, fig. 1.

References Ehrenberg 1841, pl. 1(1), fig. 11, pl. 1(3), fig. 16, pl. 2(6), fig. 10; Kützing 1844, p. 73, pl. 5, figs. VI-3, 6; Smith 1853–1856, p. 22, pl. 3, fig. 34; Van Heurck 1880–1885, p. 132, pl. 29, figs. 1–3; Wolle 1890, pl. 33, figs. 12–14, 22, 23; Schmidt et al. 1874–1959, pl. 190, figs. 17–21; Van Heurck 1896, p. 122, fig. 224a,b; Peragallo and Peragallo 1897–1908, p. 19, pl. 4, fig. 5; Frenguelli 1922–1924, p. 110, pl. 9, fig. 20; Karsten 1928, p. 271, fig. 360a,b; Frenguelli 1930, p. 267, pl. 2, fig. 4; Hustedt 1930, p. 191, fig. 267; Hustedt 1959, p. 337, fig. 790 (Figure 1); Okuno 1957, p. 221, pl. 7, fig. 1a–f; Hendey 1964, p. 180, pl. 27, fig. 8; Rivera et al. 1973, p. 28, pl. 6, figs. 19, 20; Montgomery and Miller 1978, pl. 66, figs. e, f; Riaux-Gobin and Germain 1980, pl. 1 figs. 1, 2; Holmes et al. 1982, p. 371, figs. 24–28; Navarro 1982a, p. 322, figs. 14, 15; Noel 1984, p. 88, figs. 7, 8; Poulin et al. 1984, p. 56, figs. 43–48; Mizuno 1987, p. 591, fig. 6a–f; Lange-Bertalot and Krammer 1989, pl. 1, fig. 2, pl. 2, figs. 1–6, pl. 3, figs. 1–6, pl. 4, figs. 1–5, pl. 5, fig. 5; Riaux-Gobin 1991a, p. 129, pl. 2, figs. 2–4; Mazzella et al. 1994, fig. 3b; Romero 1996, figs. 2–17; Ognjanova-Rumenova and Zapryanova 1998, pl. 3, figs. 1–9; Witkowski et al. 2000, p. 114, pl. 36, figs. 1–7, pl. 38, fig. 11.

LM and EM material Cleaned material from *Posidonia oceanica* leaves collected in the western and eastern Mediterranean Sea (Table 1).

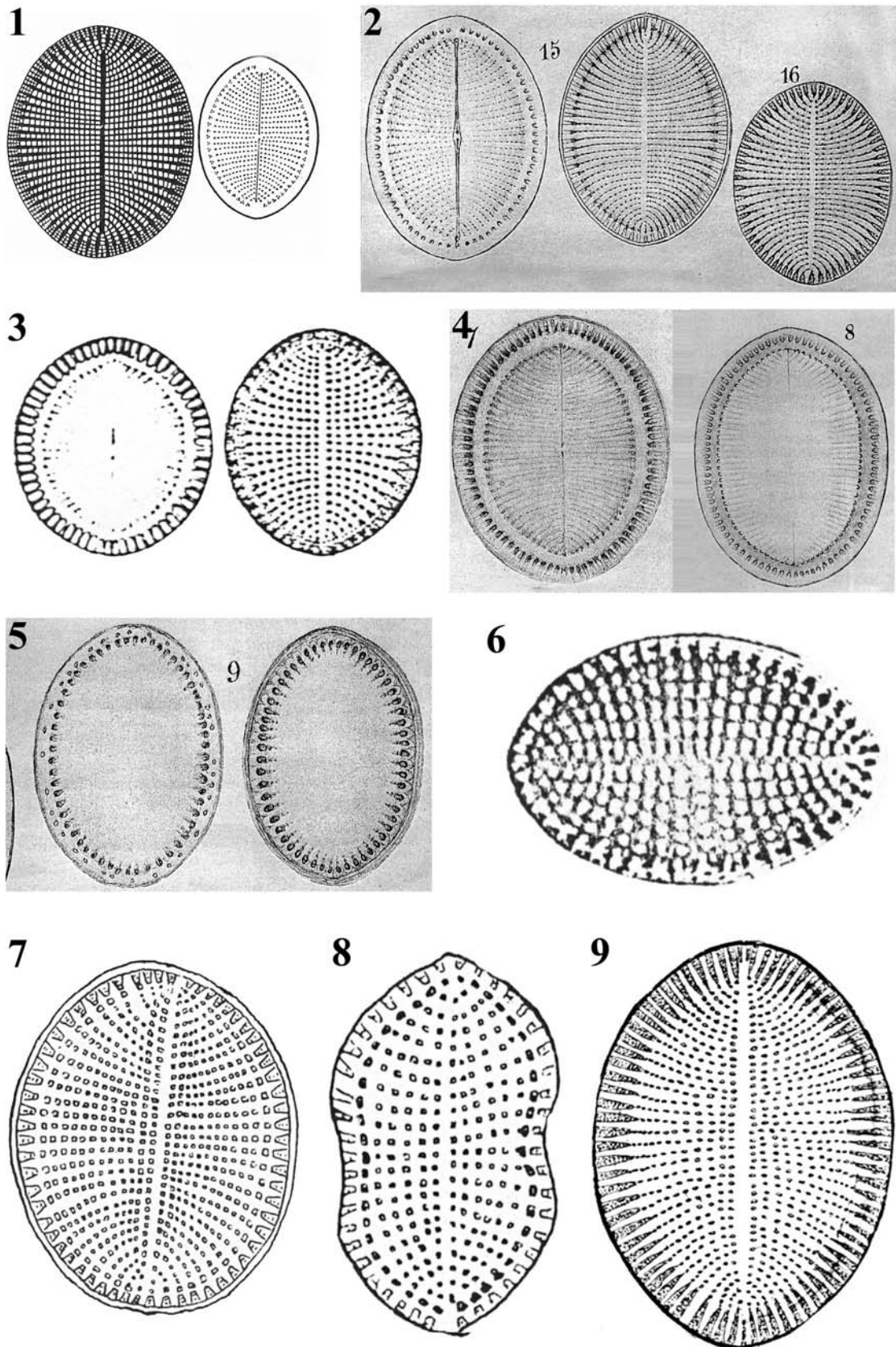
Morphology The valve outline is elliptical (Figures 19, 28). Apical axis (AA): 22–46 μm . Transapical axis (TA): 11–35 μm .

Sternum valve (SV): In external view, the valve face is flat or slightly convex and the mantle is low and smooth (Figure 20). The straight axial area lacks a central area

and almost reaches the apex (Figures 20, 24). The number of striae is 10–12 in 10 μm , uniseriate over most of the valve face (Figures 20, 21) and gradually becoming bi- to triseriate near the mantle where they are bordered by a narrow marginal hyaline area (Figure 20). Interstriae are clearly visible and of a similar width (Figure 21). Most of the valve face is perforated by poroid areolae, 14–16 in 10 μm , which are arranged in an apically oriented pattern (Figures 20, 24). The poroid areolae are circular and internally occluded by thin hymenes with linear perforations of different length that are radially distributed at the margin (Figures 22, 23). The internal valve face has the same structure as the external face with, however, a stronger silicification of the axial area and interstriae (Figures 26, 27). The valvocopula is closed and bears short fimbriae that are connected with the interstriae at the valve margin; both advalvar and abvalvar edges of the valvocopula are smooth (Figure 25).

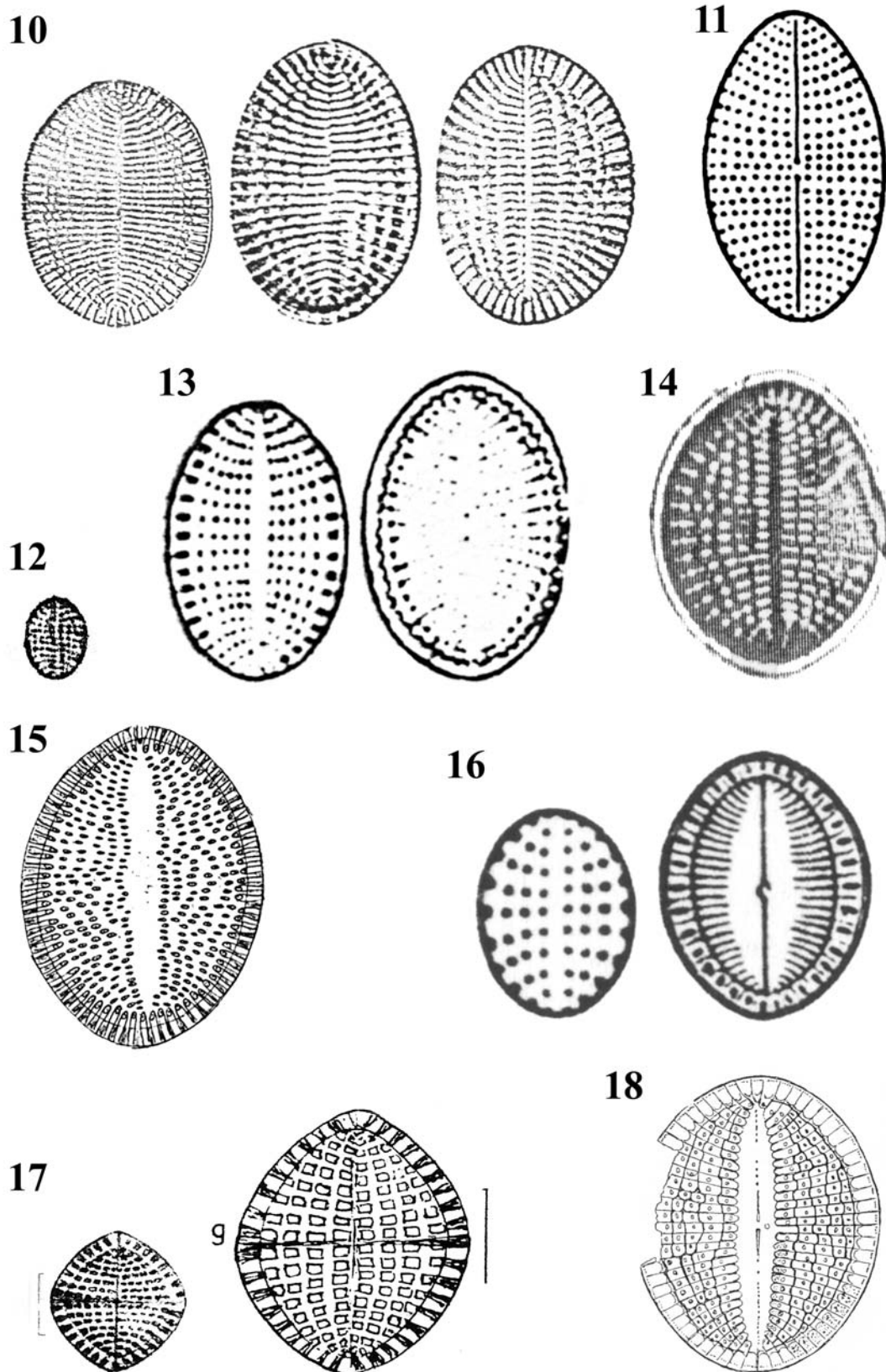
Raphe-sternum valve (RSV): Externally, the flat to concave valve face is separated from a short and slightly concave mantle (Figures 29, 34) by a narrow submarginal hyaline area (Figure 29, arrow). The raphe consists of two straight and thin fissures, with coaxial reduced proximal endings (Figure 32) and slightly broadened distal endings in the submarginal area (Figure 29). Striae are radiate, 10–13 in 10 μm , and uniseriate from the valve centre to the submarginal hyaline area (Figures 29, 34), becoming biseriate on the mantle (Figures 29, 31). Each stria is composed of circular poroids, 16–18 in 10 μm , occluded externally by hymenes with radially arranged perforations of different length (Figure 30). Internally, the submarginal hyaline area is thickened and slightly raised, bearing apically elongated bumps approximately every two interstriae (Figure 33, arrows). The internal raphe branches have proximal endings gently deflected in opposite directions, converging in a small, rounded and strongly silicified central nodule (Figure 33), and straight and slightly raised distal endings in small helictoglossae (Figure 31). The closed valvocopula bears short fimbriae (Figure 35) that extend over the thickened, submarginal hyaline area between each pair of apically elongated bumps (Figure 35, arrows). Roundish papillae covered by parallel transverse furrows are located in the basal portion of the abvalvar surface of most of the fimbriae (Figure 35, arrowhead). The advalvar surface of the valvocopula is smooth.

Taxonomic remarks *Cocconeis scutellum* was introduced by Ehrenberg (1837, p. 173) together with *C. undulata*, but the descriptions of the two taxa were erroneously pooled making its nomenclatural status invalid according to the International Code of Botanical Nomenclature (Greuter et al. 2000). In 1838, Ehrenberg provided a valid description of *C. scutellum* including cell size (22–106 μm) and stria density on the sternum valve (4.7–6.1 in 10 μm), and he considered this taxon as the type species for the genus *Cocconeis*. The main taxonomic feature circumscribing *C. scutellum* is the poroidal arrangement of the areolae, which is uniseriate on most of the valve face, becoming bi- or triseriate on the mantle (Cleve 1895, Peragallo and Peragallo 1897–1908, Hustedt 1959, Hendey 1964, Holmes et al. 1982, Poulin et



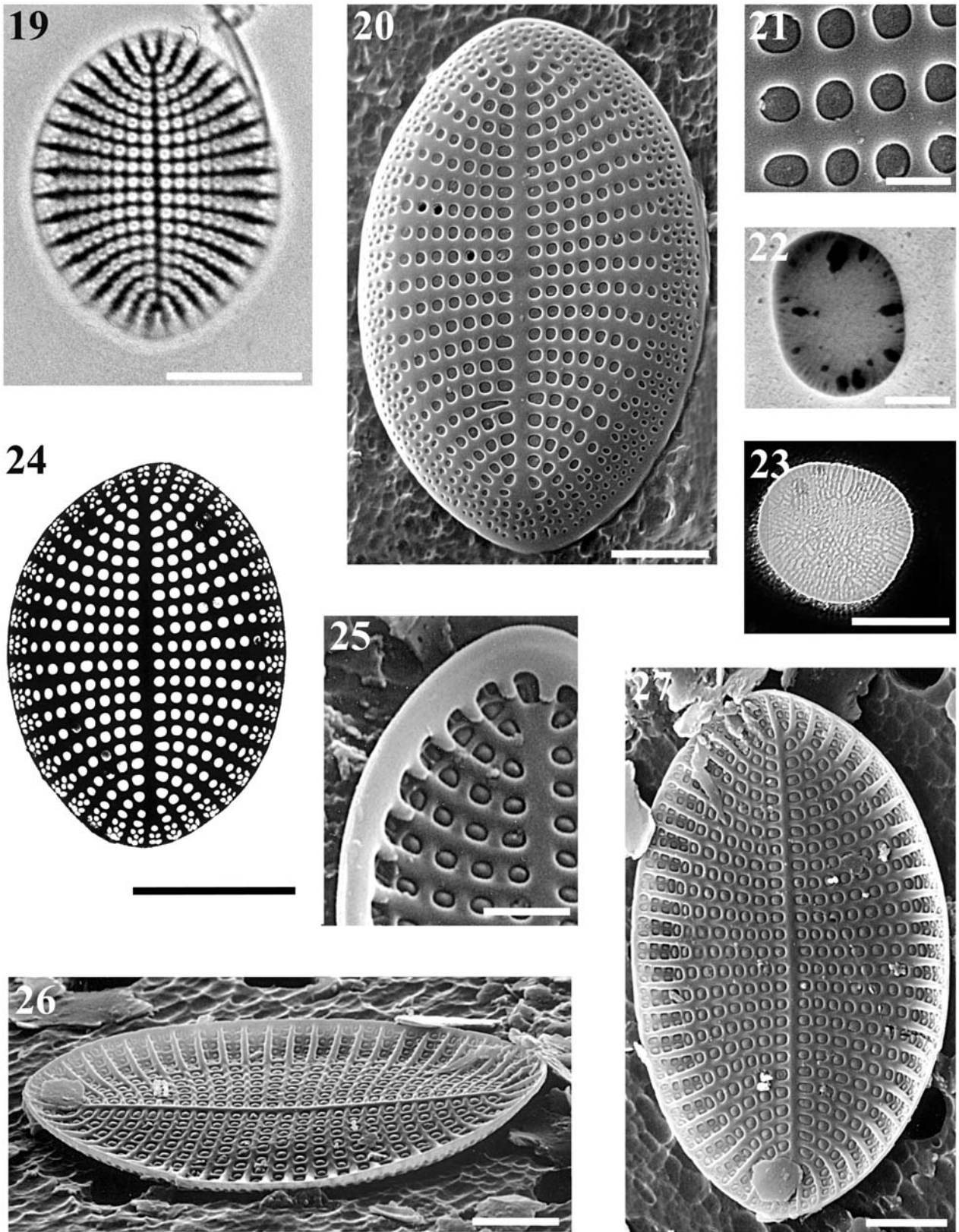
Figures 1–9 Original drawings of *Cocconeis scutellum* and varieties.

(1) Sternum and raphe-sternum valves of *C. scutellum* var. *scutellum* from Hustedt 1959. (2) Raphe-sternum and two sternum valves of *C. adjuncta* from Schmidt et al. 1874–1959. (3) Raphe-sternum and sternum valves of *C. scutellum* var. *adjuncta* from Peragallo and Peragallo 1897–1908. (4) Raphe-sternum valve and a complete frustule of *C. baldjikiana* from Schmidt et al. 1874–1959. (5) Two valvocopulae of *C. baldjikiana* from Schmidt et al. 1874–1959. (6) Sternum valve of *C. scutellum* var. *bipunctata* from Missuna 1913. (7) Sternum valve of *C. scutellum* var. *clinoraphis* from Zanon 1948. (8) Sternum valve of *C. scutellum* var. *constricta* from Zanon 1948. (9) Internal view of sternum valve of *C. scutellum* var. *doljensis* from Pantocsek 1886–1903.



Figures 10–18 Original drawings of various taxa of *Cocconeis scutellum*.

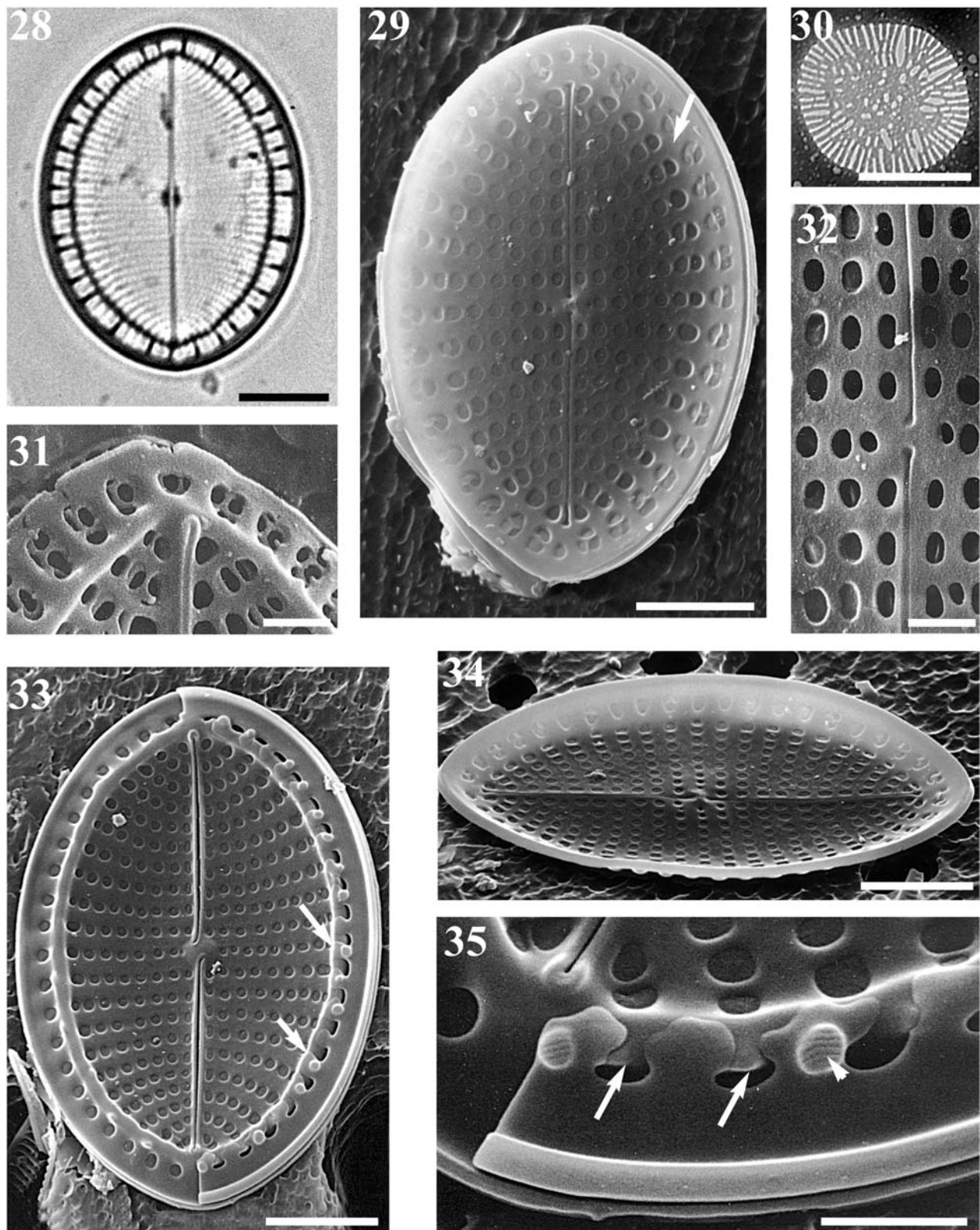
(10) Three sternum valves of *C. scutellum* var. *inequalepunctata* from Missuna 1913. (11) Raphe-sternum valve of *C. scutellum* var. *japonica* from Skvortzow 1929. (12) Sternum valve of *C. scutellum* var. *minutissima* from Van Heurck 1880–1885. (13) Sternum and raphe-sternum valves of *C. scutellum* var. *parva* from Peragallo and Peragallo 1897–1908. (14) Sternum valve of *C. scutellum* var. *pulchra* from Missuna 1913. (15) Sternum valve of *C. scutellum* var. *raeana* from Pantocsek 1889–1903. (16) Sternum and raphe-sternum valves of *C. scutellum* var. *schmidtii* from Frenguelli 1930. (17) Sternum valves of *C. scutellum* var. *speciosa* from Cleve-Euler 1953. (18) Entire frustule of *C. scutellum* var. *scutellum* f. *birhaphidea* from Jurilj 1957.



Figures 19–27 Sternum valves of *Cocconeis scutellum* var. *scutellum*.

(19) Complete valve. (20) External view of the valve. (21) Detail of the external striation on the valve face. (22) External detail of a hymenate poroid on the valve face. (23) Fine structure of a valve face poroid showing the thin hymen with linear perforations of different length, radially distributed at the margin. (24) Complete valve. (25) Internal view of the valve showing the fimbriate valvocopula. (26) Internal valve surface at 60° tilt. (27) Internal view of the valve.

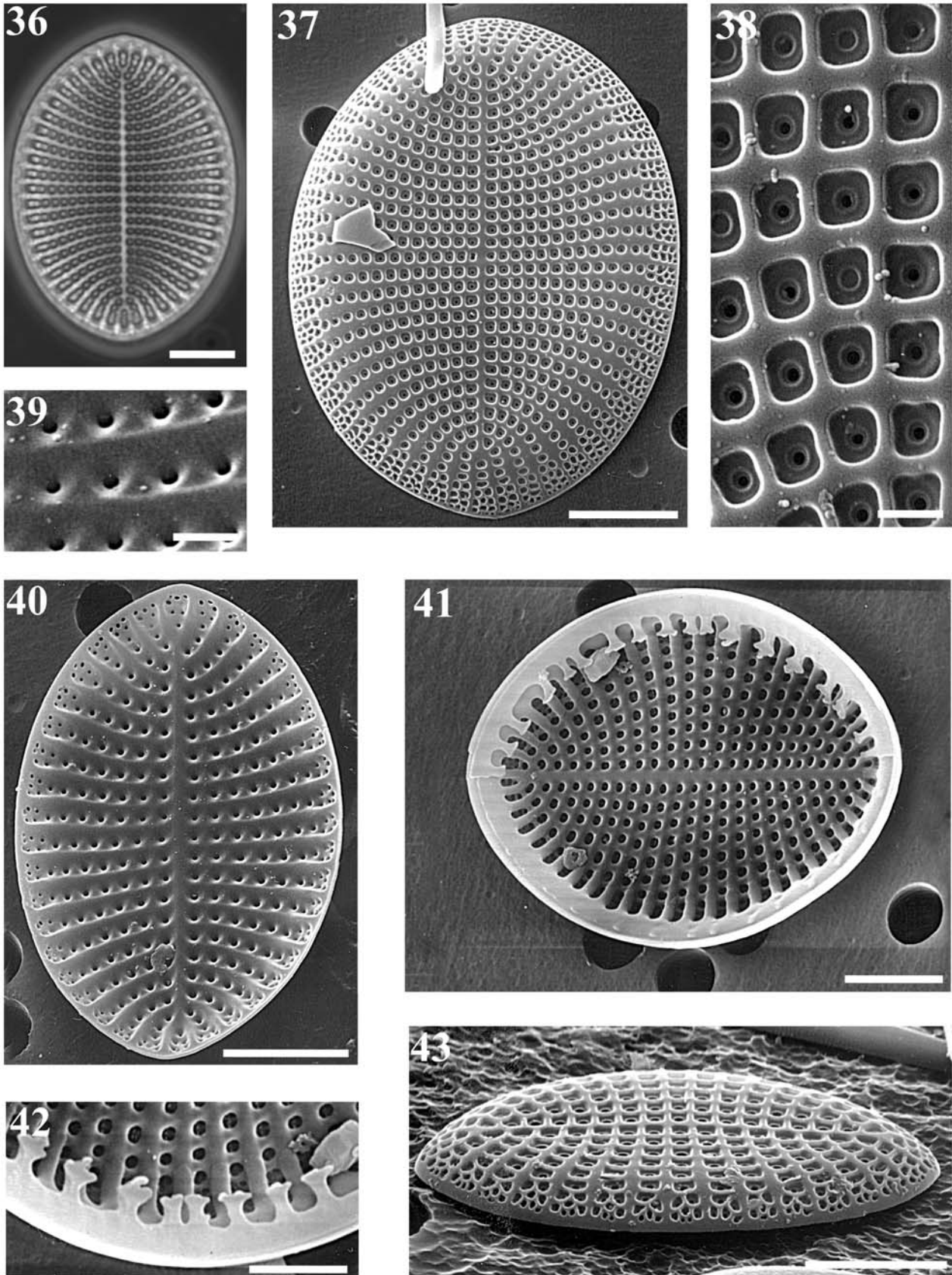
Figure 19, LM; Figures 20–23, 25–27, SEM; Figure 24, TEM. Scale bars=10 μm (Figures 19, 24); 5 μm (Figures 20, 26, 27); 2 μm (Figure 25); 1 μm (Figure 21); 0.3 μm (Figure 23); 0.2 μm (Figure 22).



Figures 28–35 Raphe-sternum valves of *Cocconeis scutellum* var. *scutellum*.

(28) Complete valve. (29) External view of the valve showing the submarginal hyaline area (arrow). (30) Fine detail of a poroid areola showing the thin hymen with linear perforations of different length, radially distributed at the margin. (31) Internal terminal raphe ending with helictoglossa. (32) External coaxial proximal raphe endings. (33) Internal view of the valve showing the slightly deflected central raphe endings and the central nodule. Note the submarginal hyaline area (arrows) separating the mantle from the valve face. (34) External valve surface at 60° tilt. (35) Internal view of the valve showing the valvocopula. Arrows indicate bumps of the thickened, submarginal area and arrowhead points to a roundish papilla covered by transverse furrows located in the basal portion of the abvalvar surface of fimbriae.

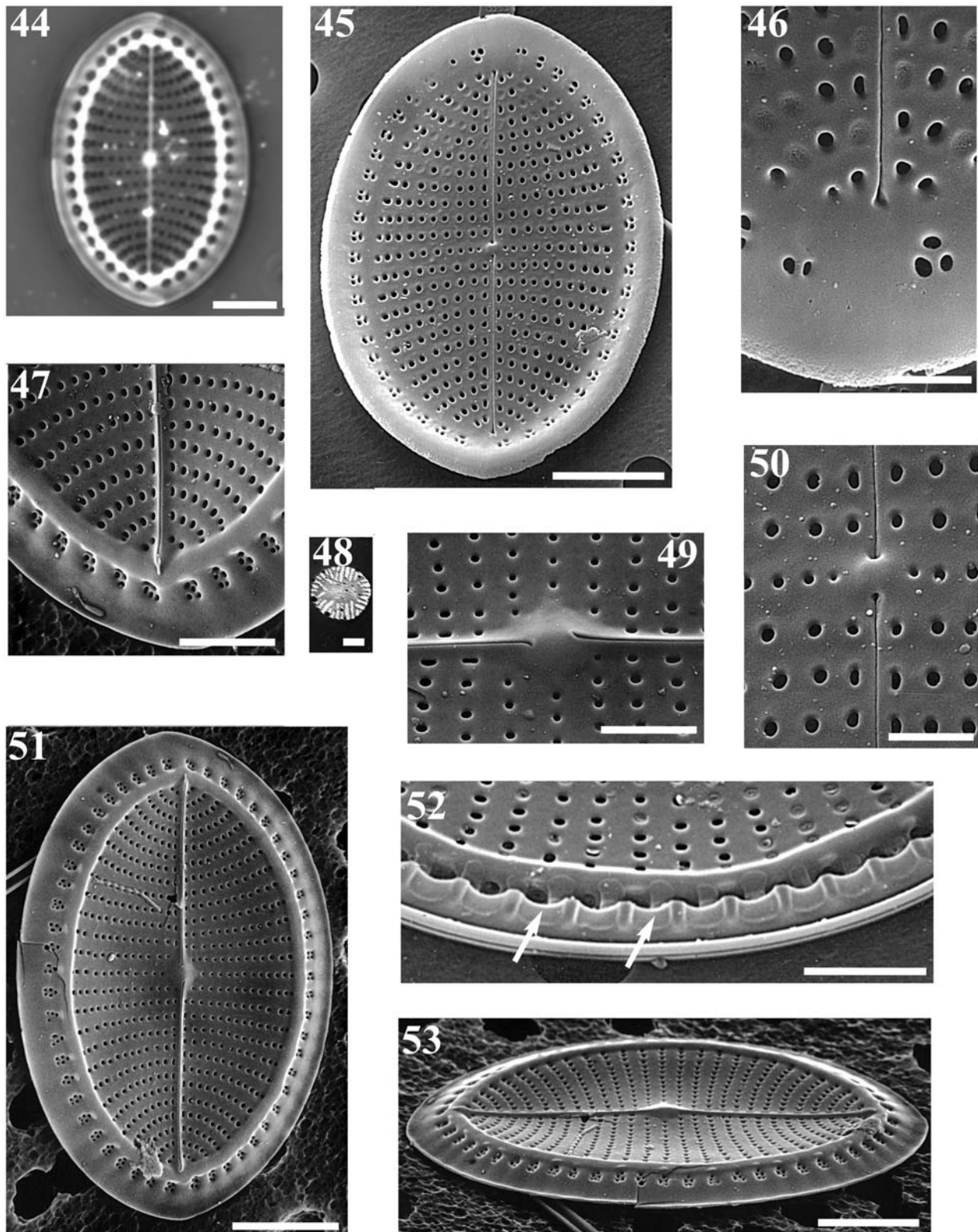
Figure 28, LM; Figures 29, 31–35, SEM; Figure 30, TEM. Scale bars=10 μm (Figure 28); 5 μm (Figures 29, 33, 34); 1 μm (Figures 31, 32, 35); 0.2 μm (Figure 30).



Figures 36–43 Sternum valves of *Cocconeis scutellum* var. *baldjikiana*.

(36) Complete valve. (37) External view of the valve. (38) Poroid areolae in external view. Note the thickened quadrangular margins and internal hymenes with a central foramen. (39) Poroid areolae in internal view. (40) Internal view of the valve. (41) Internal view of the valve showing closed valvocopula with digitiform fimbriae expanded in lateral lobes. (42) Detail of the digitiform fimbriae. (43) External valve surface at 60° tilt.

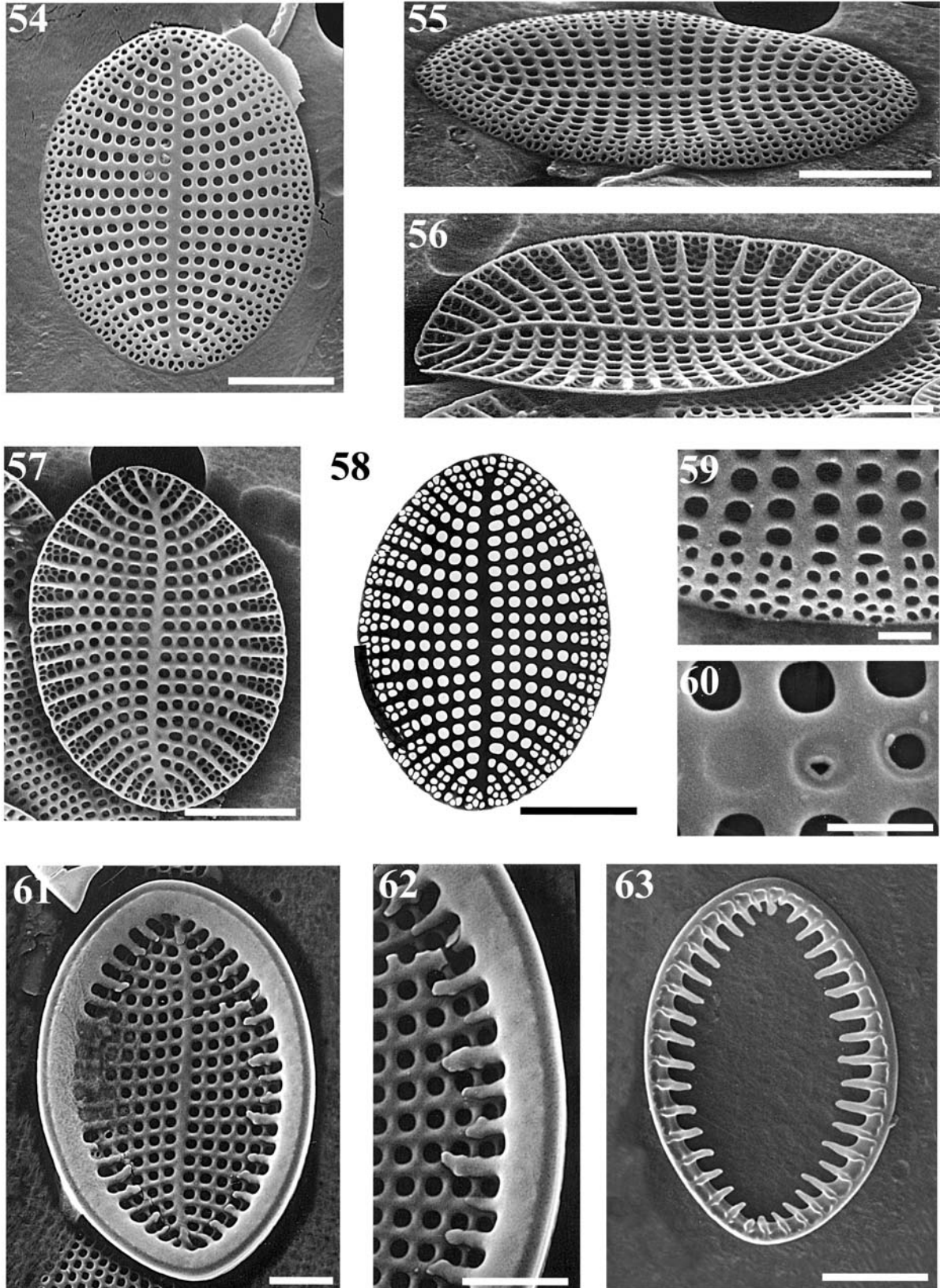
Figure 36, LM; Figures 37–43, SEM. Scale bars=10 µm (Figures 36, 37, 40, 41, 43); 5 µm (Figure 42); 2 µm (Figure 39); 1 µm (Figure 38).



Figures 44–53 Raphe-sternum valves of *Cocconeis scutellum* var. *baldjikiana*.

(44) Complete valve. (45) External view of the valve. (46) Detail of a drop-shaped distal raphe ending in external view. (47) Internal terminal raphe ending with helictoglossa. (48) Detail of a poroidal hymen having linear perforations of different length, radially distributed at the margin. (49) Central raphe endings and central nodule in internal view. (50) Drop-shaped external proximal raphe endings. (51) Internal view of the valve. Note the submarginal hyaline area separating the mantle from the valve face. (52) Detail of the valve mantle with the attached valvocopula overlaid by the SV valvocopula. Arrows indicate fimbriae of SV valvocopula. (53) Internal valve surface at 60° tilt.

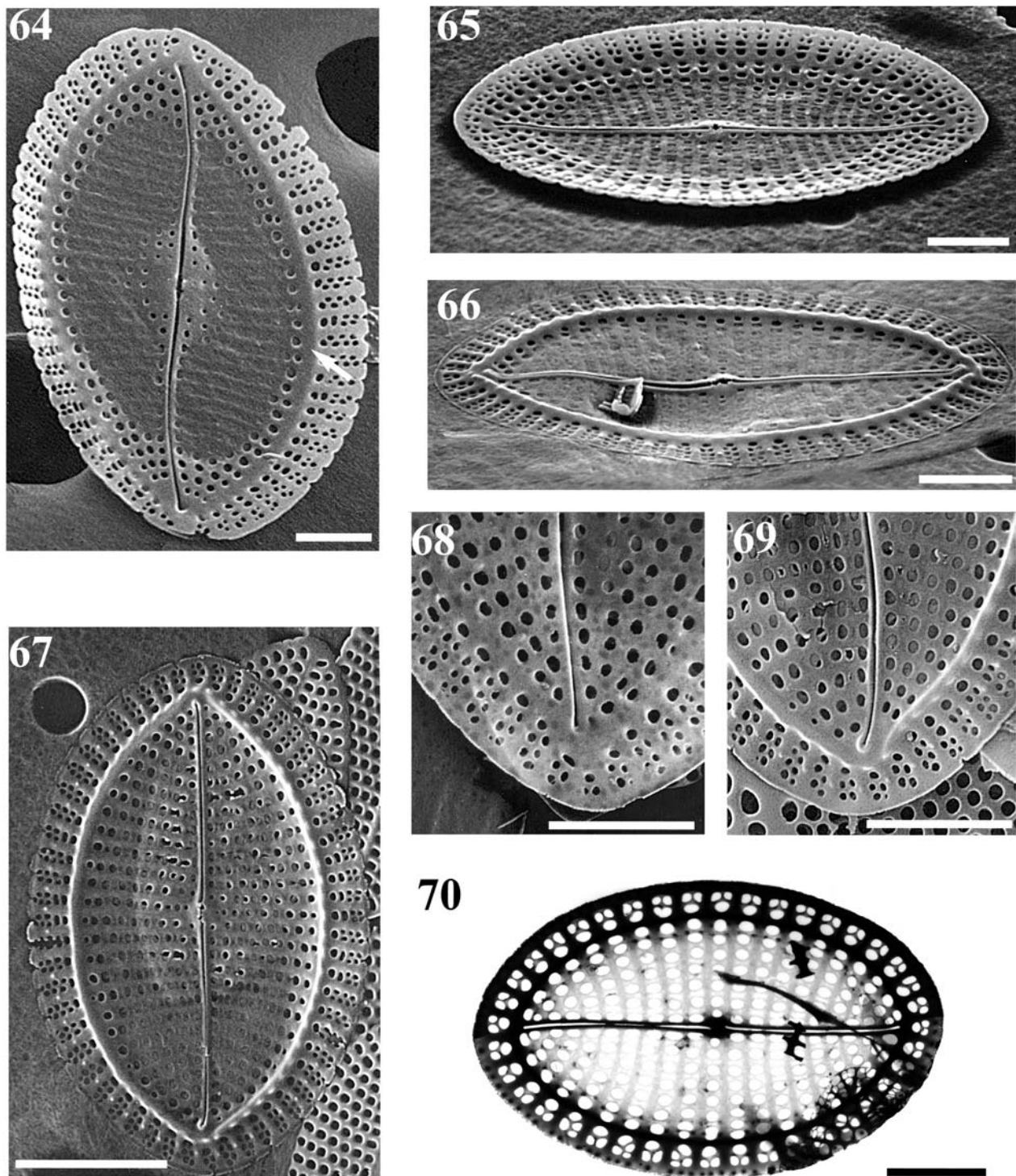
Figure 44, LM; Figures 45–47, 49–53, SEM; Figure 48, TEM. Scale bars=10 μm (Figures 44, 45, 51, 53); 5 μm (Figures 47, 52); 2 μm (Figures 46, 49, 50); 0.1 μm (Figure 48).



Figures 54–63 Sternum valves of *Cocconeis scutellum* var. *clinoraphis*.

(54) External view of the valve showing the sigmoid sternum. (55) External view of the valve at 60° tilt showing the slightly concave valve surface. (56) Internal valve view at 60° tilt. (57) Internal view of the valve. Note the absence of a submarginal hyaline area. (58) Complete valve. (59) Detail of uniseriate striae on the valve face becoming bi- to triseriate on the mantle. (60) Detail of large circular poroid areolae occluded by hymenes. (61) Internal view showing the closed valvocopula. (62) Advalvar view of the valvocopula with digitiform fimbriae connected to interstriae. (63) Closed valvocopula.

Figures 54–57, 59–63, SEM; Figure 58, TEM. Scale bars=10 μm (Figures 54, 55, 57, 58, 63); 5 μm (Figures 56, 61, 62); 1 μm (Figures 59, 60).



Figures 64–70 Raphe-sternum valves of *Cocconeis scutellum* var. *clinoraphis*.

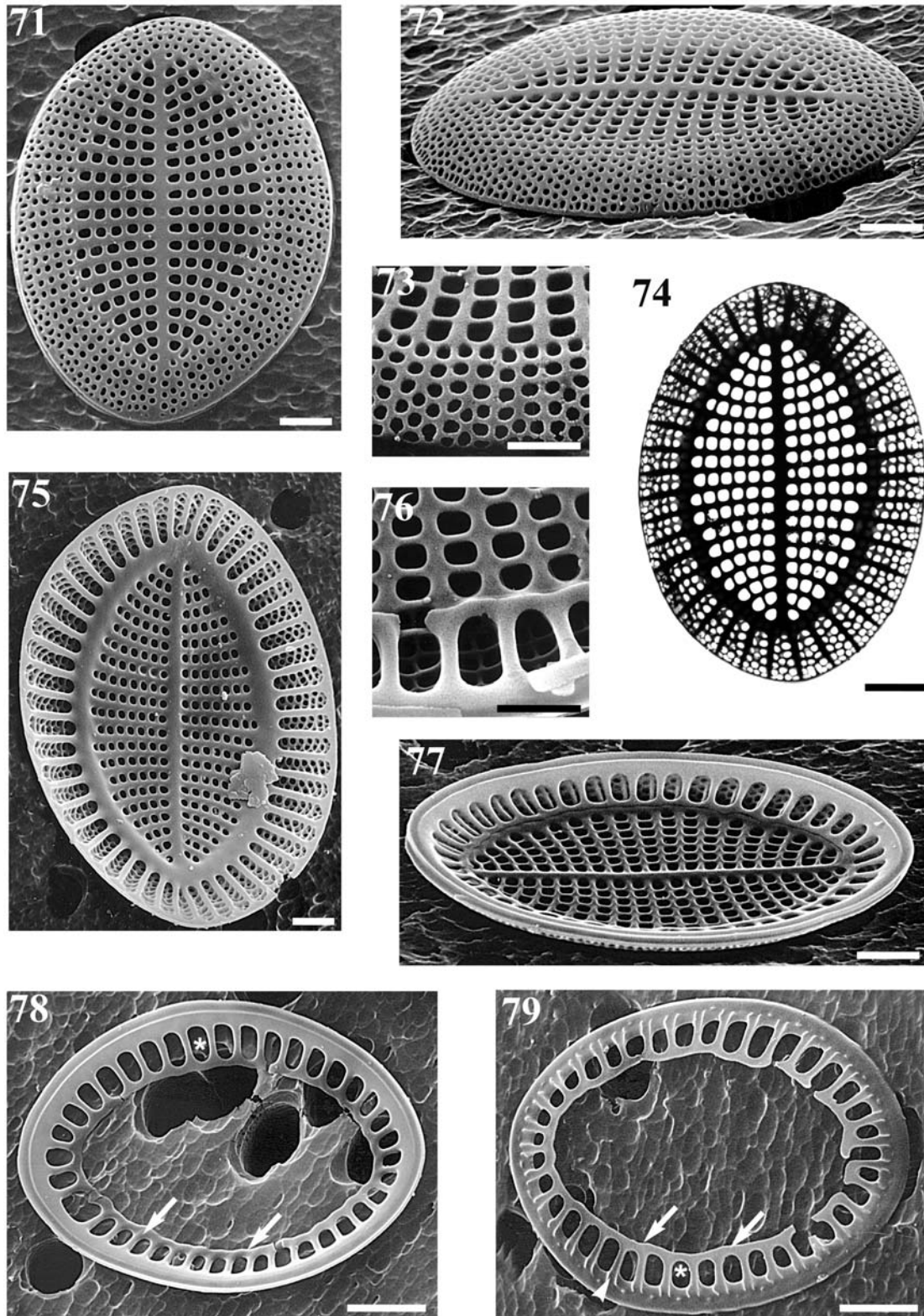
(64) External view of the valve showing the sigmoid raphe-sternum. (65) External valve view at 60° tilt showing the flat to concave valve face and proximal raphe endings. (66) Internal valve view at 60° tilt. Note the thickened submarginal hyaline area separating the valve face from the mantle. (67) Internal view of the valve showing the central raphe endings converging to the central nodule. (68) Detail of the reduced distal raphe ending in external view. (69) Distal raphe ending with helictoglossa in internal view. (70) Complete valve.

Figures 64–69, SEM; Figure 70, TEM. Scale bars=10 µm (Figure 67); 5 µm (Figures 64–66, 68–70).

al. 1984, Romero 1996, De Stefano and De Stefano 2005) (Figure 1). Furthermore, the occurrence of a loculiferous rim or a marginal band has often been reported near the valve margin (Smith 1853–1856, Van Heurck 1880–1885, 1896, Cleve 1895, Peragallo and Peragallo 1897–1908, Hustedt 1959, Hendey 1964). Both of these structures

have been identified as fimbriate valvocopulae (Holmes et al. 1982, Romero 1996, De Stefano et al. 2000, De Stefano and Marino 2003, De Stefano and De Stefano 2005).

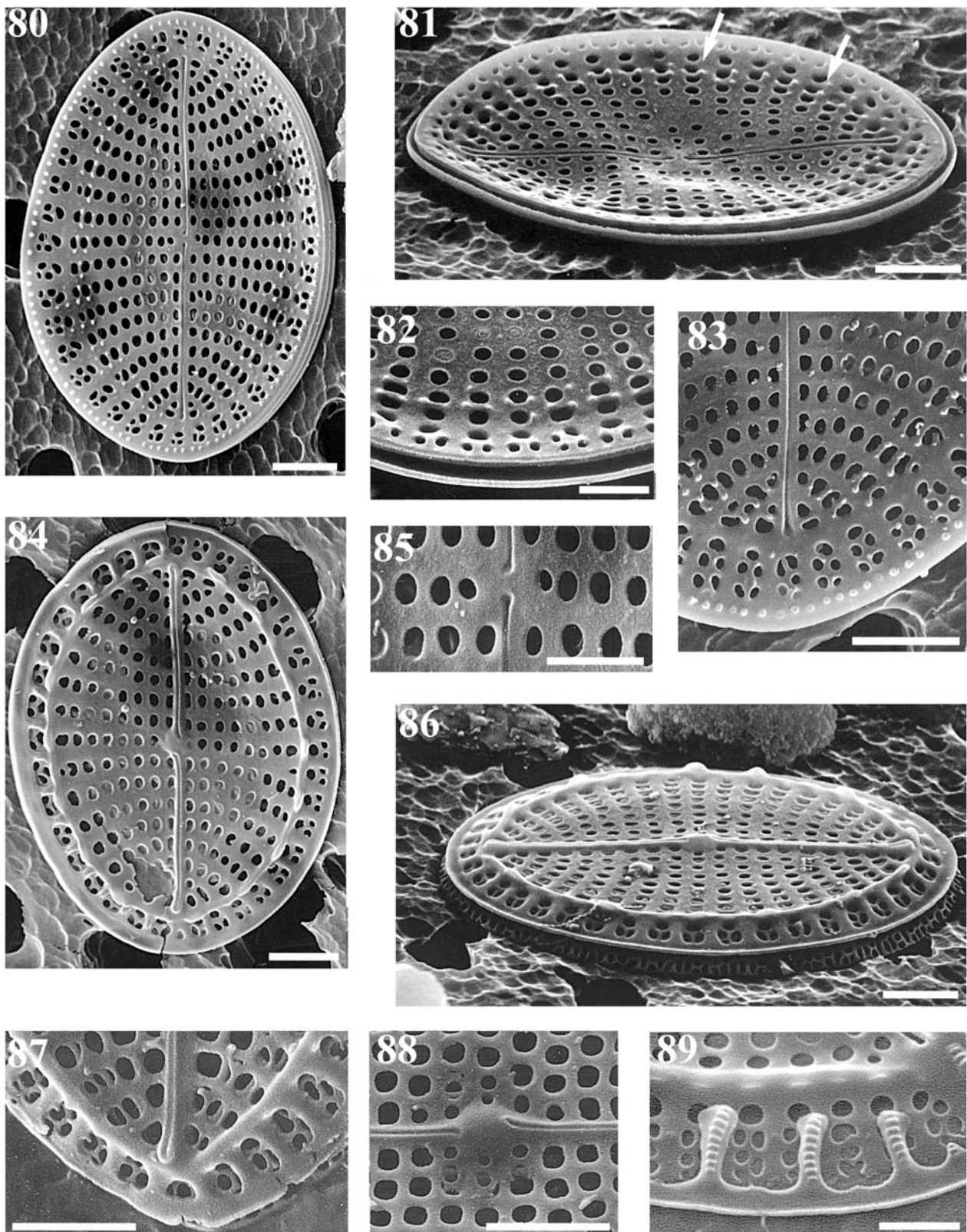
Many taxa allied to *Cocconeis scutellum* var. *scutellum* were listed by VanLandingham (1968, 1979), but most



Figures 71–79 Sternum valves of *Cocconeis scutellum* var. *gorensis*.

(71) Valve in external view. (72) External valve view at 60° tilt showing the flat valve face and the wide mantle. (73) Detail of the striation consisting of subquadrangular poroid areolae on the valve face changing to small and circular areolae on the mantle. (74) Complete valve. (75) Internal valve view with well-developed and strongly silicified submarginal hyaline area at the border between the valve face and mantle. (76) Detail of the valvocopula fimbriae showing a central rib with lobed extensions joined together with adjacent ones creating an undulated distal margin delimiting a series of quadrangular openings. (77) Internal valve view at 60° tilt showing closed fimbriate valvocopula. (78) Valvocopula in abvalvar view. Arrows indicate the undulated distal margin of the fimbriae and the asterisk points to a quadrangular opening between extended fimbriae. (79) Valvocopula in advalvar view. Arrows indicate the undulated distal margin of the fimbriae, the arrowhead shows thickenings on the margins of the central ribs of the fimbriae and the asterisk points to a quadrangular opening between extended fimbriae.

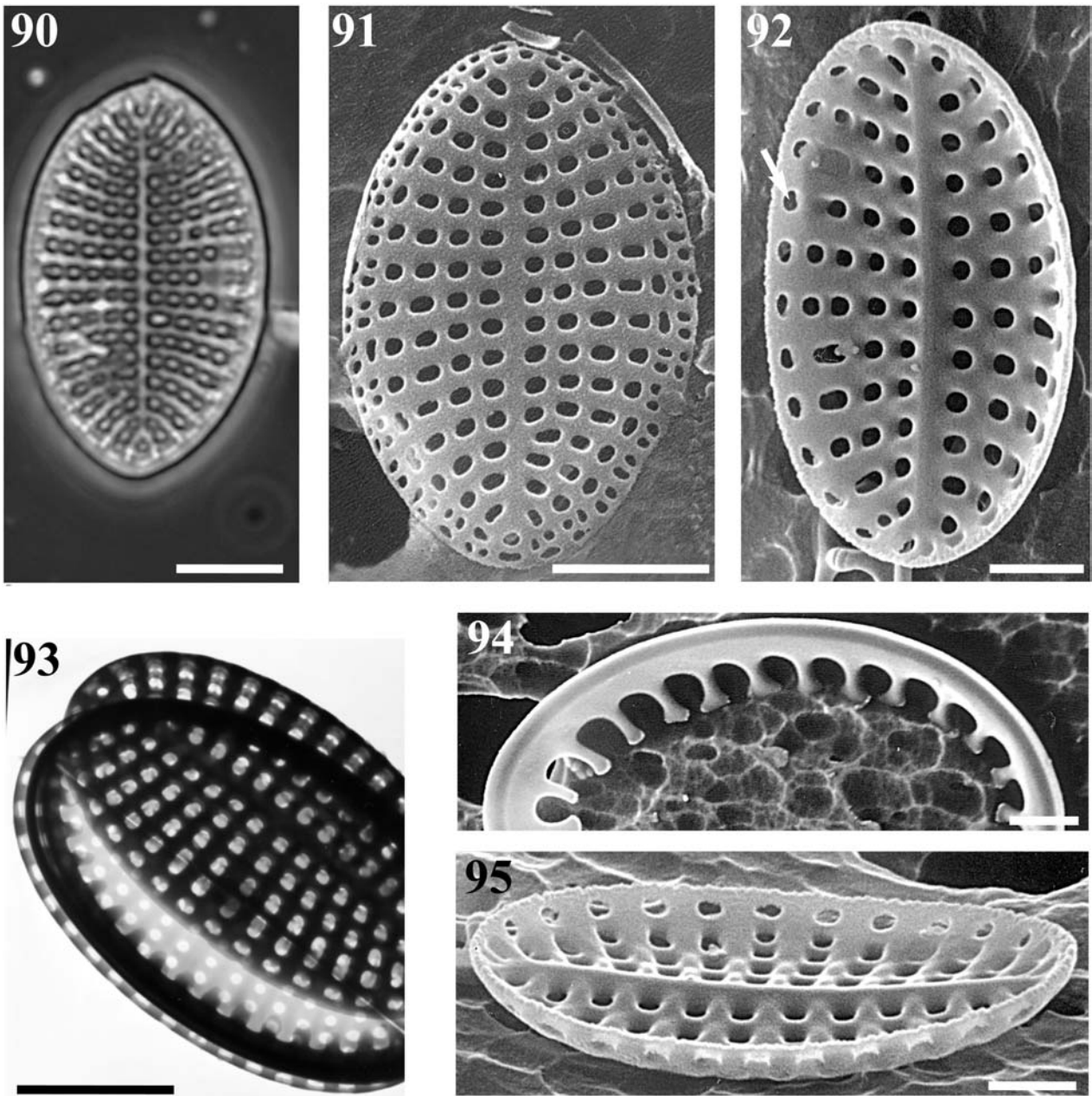
Figures 71–73, 75–79, SEM; Figure 74, TEM. Scale bars=10 μm (Figures 71, 72, 74, 75, 77–79); 5 μm (Figures 73, 76).



Figures 80–89 Raphe-sternum valves of *Cocconeis scutellum* var. *gorenensis*.

Figures 80–89, SEM. Scale bars=10 μ m (Figures 80, 81, 83, 84, 86–88); 5 μ m (Figures 82, 85, 89).

(80) External view of the valve. (81) External valve view at 60° tilt showing the flat to concave valve face. Arrows indicate the submarginal hyaline area. (82) Detail of the reduced mantle. (83) Detail of the apically expanded distal raphe ending in external view. (84) Internal view of the valve. (85) External view of proximal raphe endings. (86) Internal valve view at 60° tilt showing mantle striae. Note the thickened and slightly raised submarginal area separating the mantle from the valve face. (87) External terminal raphe ending with helictoglossa. (88) Internal central raphe endings and central nodule. (89) Digitate fimbriae of the valvocopula with apically elongated papillae covered by horizontal furrows.



Figures 90–95 Sternum valves of *Cocconeis scutellum* var. *parva*.

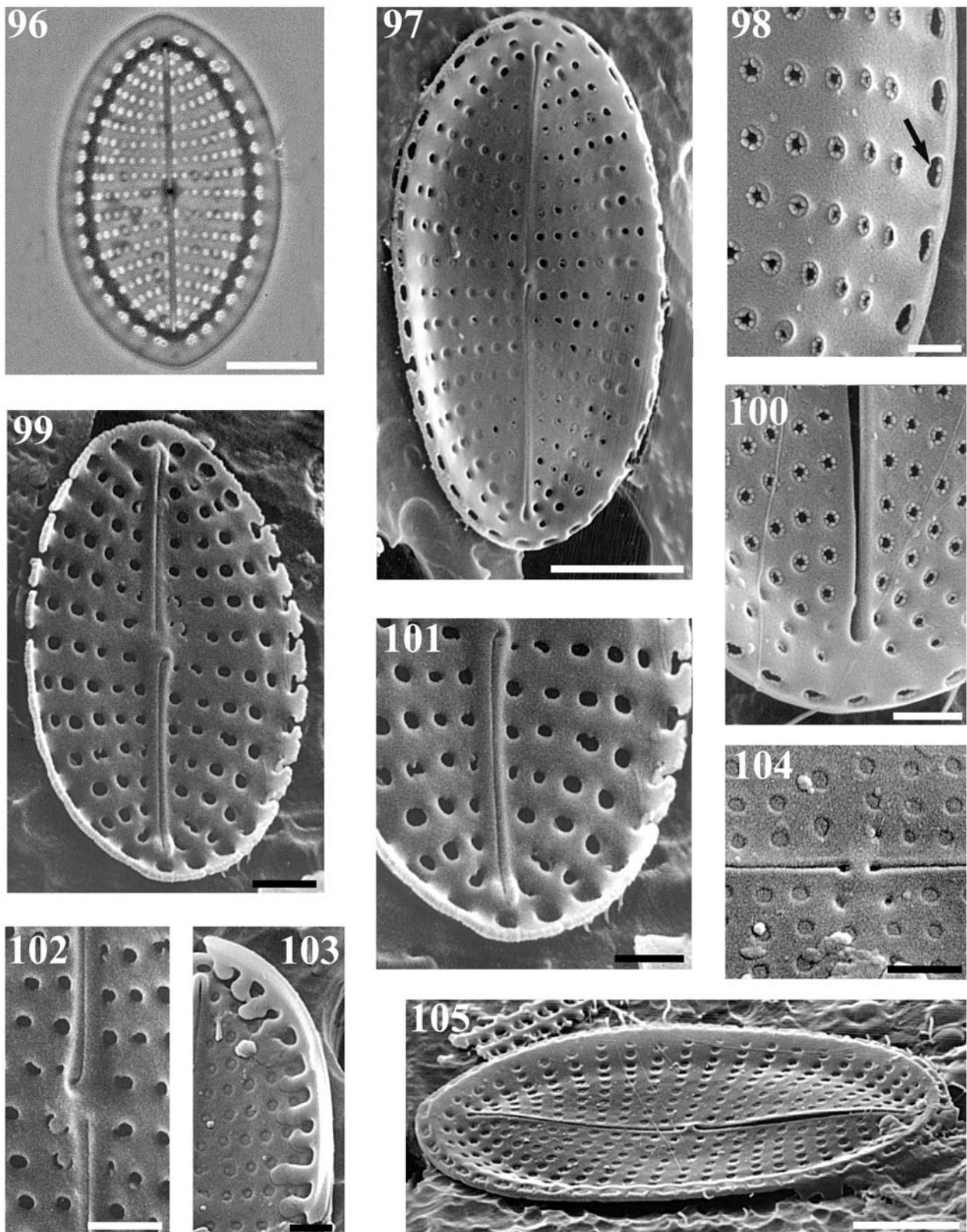
(90) Complete valve. (91) External view of the valve. (92) Internal view of the valve. Arrow indicates the large apically elongated poroid areola at the end of each stria. (93) Entire frustule with the SV valvocopula. (94) Valvocopula with digitate fimbriae. (95) Internal valve view at 60° tilt showing strongly silicified interstriae.

Figure 90, LM; Figures 91, 92, 94, 95, SEM; Figure 93, TEM. Scale bars=5 μm (Figures 90, 91, 93); 2 μm (Figures 92, 95); 1 μm (Figure 94).

were considered to be synonymous with this species by Hustedt (1959); however, 14 varieties and one form of *C. scutellum* are still reported as valid. Most of these varieties were described based on the observation of only one valve and often the diagnostic characters were merely minor differences in the overall morphology of the valves and in morphometric measurements. The main morphological characters circumscribing the *C. scutellum* varieties comprised the poroidal spacing within each stria and their arrangement within different striae, and the variability in the width of the interstriae and poroids.

In a morphological study of *Cocconeis scutellum*, Mizuno (1987) showed that the stria density (as in many

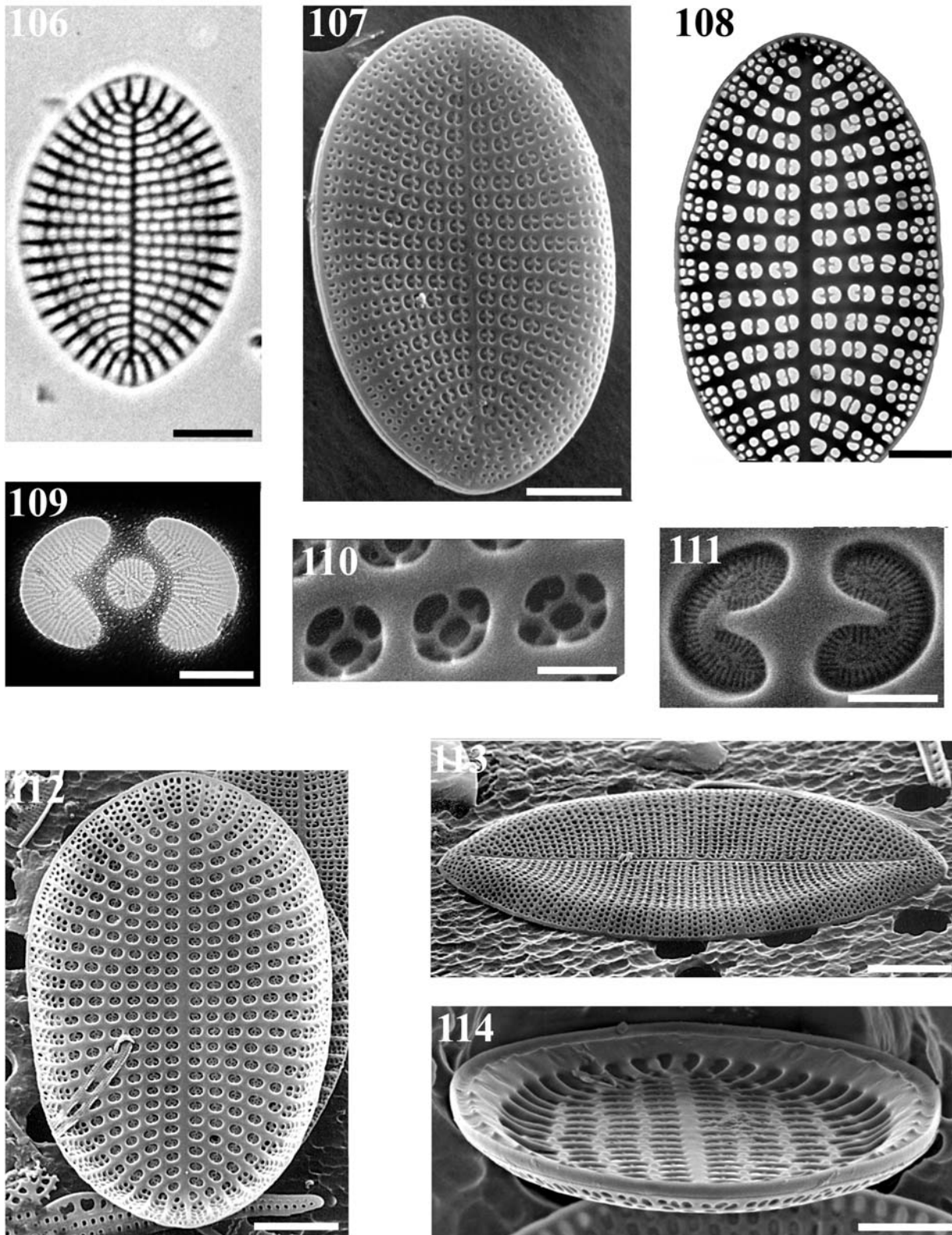
diatom species) increases from 7–9 to 9.5–12 in 10 μm in SV and 7.5–11 to 10–13.5 in 10 μm in RSV, with size reduction of the valves decreasing from 50 to 25 μm. Therefore, he suggested using simple mathematic relationships between the apical and transapical axes and the stria densities to separate *scutellum* varieties in three morphometric ranges including: 1) varieties with morphometric parameters matching those reported by Ehrenberg (1838), 2) varieties with greater valve dimensions and lower stria density than (or equal) to those reported by Ehrenberg (1838), and 3) varieties with larger valve dimensions and lower stria density only in the SV. Therefore, following Mizuno (1987), *C. scutellum* var. *doljensis*



Figures 96–105 Raphe-sternum valves of *Cocconeis scutellum* var. *parva*.

(96) Complete valve. (97) External view of the valve. (98) Detail of the large apically elongated poroid areola at the end of each stria (arrow). (99) Internal view of the valve. Note the absence of a submarginal hyaline area. (100) Drop-shaped distal raphe ending in external view. (101) Internal terminal raphe ending with helictoglossa. (102) Central raphe endings in internal view. (103) Valvocopula showing the irregularly lobate fimbriae lacking basal papillae. (104) Detail of the external central raphe endings. (105) External valve view at 60° tilt showing the reduced and low mantle.

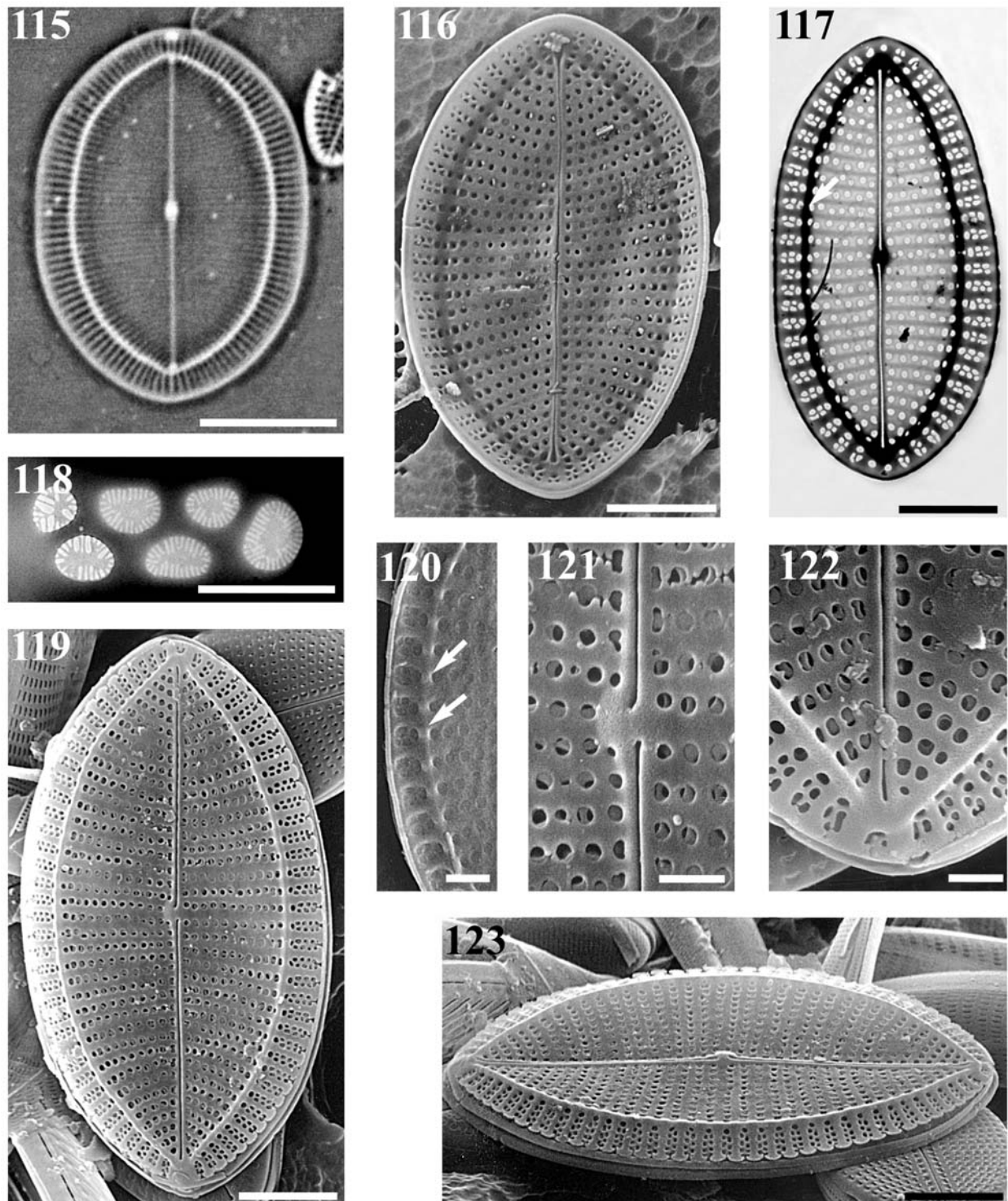
Figure 96, LM; Figures 97–105, SEM. Scale bars=5 µm (Figures 96, 97, 105); 2 µm (Figures 99–104); 1 µm (Figure 98).



Figures 106–114 Sternum valves of *Cocconeis scutellum* var. *posidoniae*.

(106) Complete valve. (107) Valve in external view. (108) Complete valve. (109) Valve face poroid areola showing the pierced rota and hymen with linear perforations of different length radially distributed on the margin. (110) Internal view of a stria showing subquadrangular poroid areolae occluded by rotate hymenes showing a pierced, wide central area. (111) External view of a poroid areola showing the tridimensional structure of the hymenes. (112) Internal view of the valve. (113) External valve view at 60° tilt. Note the slightly depressed sternum and the wide and smooth mantle. (114) Internal valve view at 80° tilt showing strong silicified interstriae and a ring of sharp bumps on the mantle.

Figure 106, LM; Figures 107, 110–114, SEM; Figures 108, 109, TEM. Scale bars=5 μm (Figures 106, 112, 113); 2 μm (Figures 107, 114); 1 μm (Figure 108); 0.3 μm (Figure 110); 0.1 μm (Figures 109, 111).

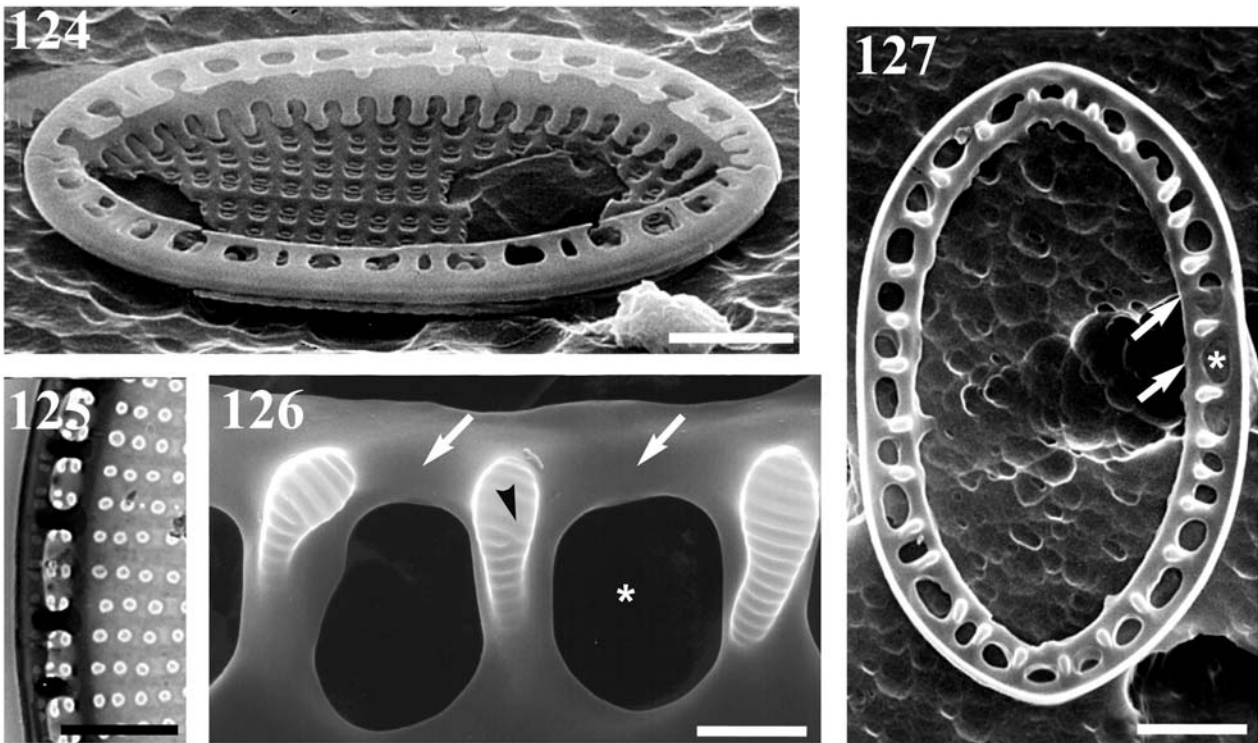


Figures 115–123 Raphe–sternum valves of *Cocconeis scutellum* var. *posidoniae*.

(115) Complete valve. (116) Valve in external view. (117) Complete valve. Arrow shows the submarginal hyaline area. (118) Circular poroid areolae on a mantle stria occluded by hymenes with linear perforations of different length radially distributed on the margin. (119) Internal view of the valve. (120) Detail of valve mantle in internal view. Arrows indicate the submarginal hyaline area appearing as an undulated rim with bumps and depressions corresponding to interstriae and striae, respectively. (121) Internal view of the central raphe endings. (122) Valve apex showing the distal raphe ending and helictoglossa. (123) Internal valve view at 60° tilt. Figure 115, LM; Figures 116, 120–123, SEM; Figures 117, 118, TEM. Scale bars=10 μm (Figure 115); 5 μm (Figures 116, 123); 2 μm (Figures 117, 119); 1 μm (Figures 120–122); 0.5 μm (Figure 118).

Pantocsek (Figure 9) and var. *raeana* (Pantocsek) Cleve (Figure 15) must be considered synonyms of the nominate variety. Both varieties were described by Pantocsek (1886–1903) based, unfortunately, on examination of a

single SV, and they shared with the nominate variety a similar valve outline, poroidal areolar shape and morphometric parameters. The diagnostic features of these two varieties mainly comprised the arrangement of the are-



Figures 124–127 Sternum and raphe-sternum valvocopulae of *Cocconeis scutellum* var. *posidoniae*.

(124) Sternum valve with two valvocopulae attached; SV valvocopula bears digitate fimbriae merging with the interstriae at margin. (125) Detail of the RSV valvocopula showing the *pars interior* extending over the thickened submarginal hyaline area. (126) Detail of the RSV fimbriate valvocopula. Arrows indicate the distal margin generated by the fusion of lobes of each fimbria, the arrowhead points to the papilla on each fimbria and the asterisk shows the interfimbrial space reduced to a large quadrangular opening. (127) Valvocopula in abvalvar view showing the distal margin generated by the fusion of lobes of each fimbria (arrows) and the interfimbrial space reduced to a large quadrangular opening (asterisk).

Figures 124, 126, 127, SEM; Figure 125, TEM. Scale bars=5 μm (Figures 124, 127); 2 μm (Figure 125); 1 μm (Figure 126).

olae in undulating longitudinal lines and the presence of a wide and lanceolate sternum in var. *raeana* only (Pantocsek 1886–1903) (Figures 9, 15). The absence of type material or current reports of this taxa precluded a sound comparison with the nominate variety, but the diagnostic characteristics of these two taxa can be viewed as transitional morphological variations.

Our observations of the valve morphology and associated ultrastructure of *Cocconeis scutellum* var. *scutellum* resembled those previously reported in the literature (Holmes et al. 1982, Poulin et al. 1984, Mizuno 1987, Lange-Bertalot and Krammer 1989, Romero 1996), but our biometric data for striae (SV: 10–12/10 μm ; RSV: 10–13/10 μm) and areolae (SV: 14–16/10 μm ; RSV: 16–20/10 μm) were slightly higher on both valves than the values usually reported for the species (Hustedt 1959, Mizuno 1987, Romero 1996).

Distribution *Cocconeis scutellum* var. *scutellum* is a cosmopolitan species, commonly occurring in epibenthic diatom populations. The species is recorded from Eurasia and North America (Ehrenberg 1838, 1841, Kützing 1844, Smith 1853–1856, Van Heurck 1880–1885, 1896, Schmidt et al. 1874–1959, Peragallo and Peragallo 1897–1908, Hustedt 1930, 1959, Okuno 1957, Hende 1964, Riaux-Gobin and Germain 1980, Poulin et al. 1984, Lange-Bertalot and Krammer 1989, Riaux-Gobin 1991a,b, Mazzella et al. 1994, Witkowski et al. 2000)

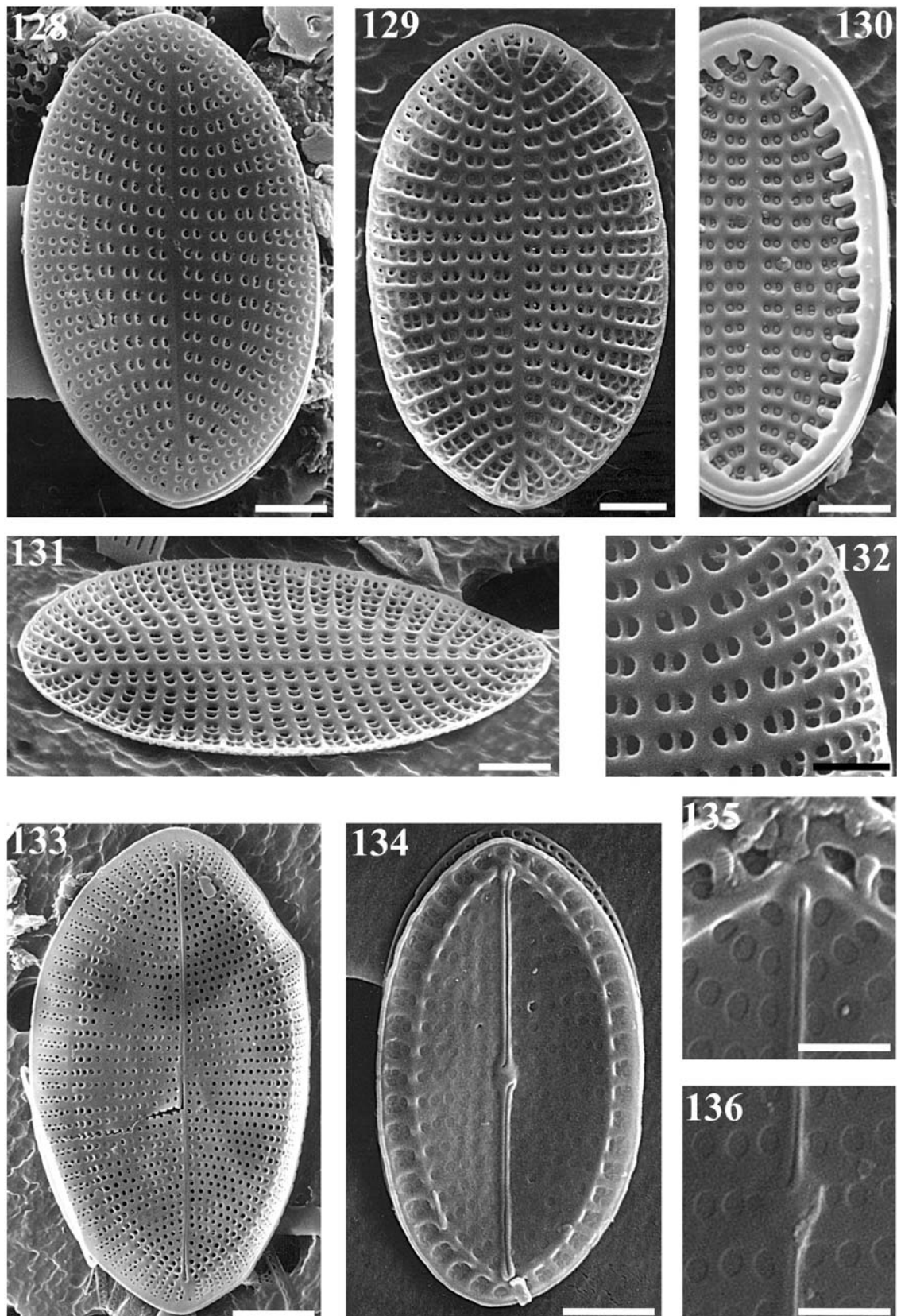
to Subantarctic and Antarctic regions (Frenguelli 1922–1924, 1930, Cholnoky 1963, Rivera et al. 1973, Rivera 1983, Romero 1996, Riaux-Gobin and Romero 2003, Sar et al. 2003) and subtropical to equatorial areas (Foged 1975, 1978, 1984, 1987, Ricard 1977, Sullivan 1979, 1981, 1982, Giffen 1980, Navarro 1982a,b). In the Mediterranean Sea, this species has been recorded from early (Rabenhorst 1864, Zanon 1948, Hustedt 1959) and more recent collections (Foged 1986, Mazzella et al. 1994, Ognjanova-Rumenova and Zaprianova 1998, Witkowski et al. 2000, De Stefano 2001) (Table 1). In the Mediterranean Sea, *C. scutellum* var. *scutellum* is always present as epiphyte on leaves of *Posidonia oceanica*, *Cymodocea nodosa* and *Zostera noltii*, although never dominant.

***Cocconeis scutellum* var. *baldjikiana* (Grunow) Cleve (Figures 36–53)**

Basionym *Cocconeis scutellum* var. *baldjikiana* Grunow 1888, p. 324.

Synonym *Cocconeis baldjikiana* Grunow 1894 in Schmidt et al. 1874–1959, pl. 190, figs. 7–10 (Figures 4, 5).

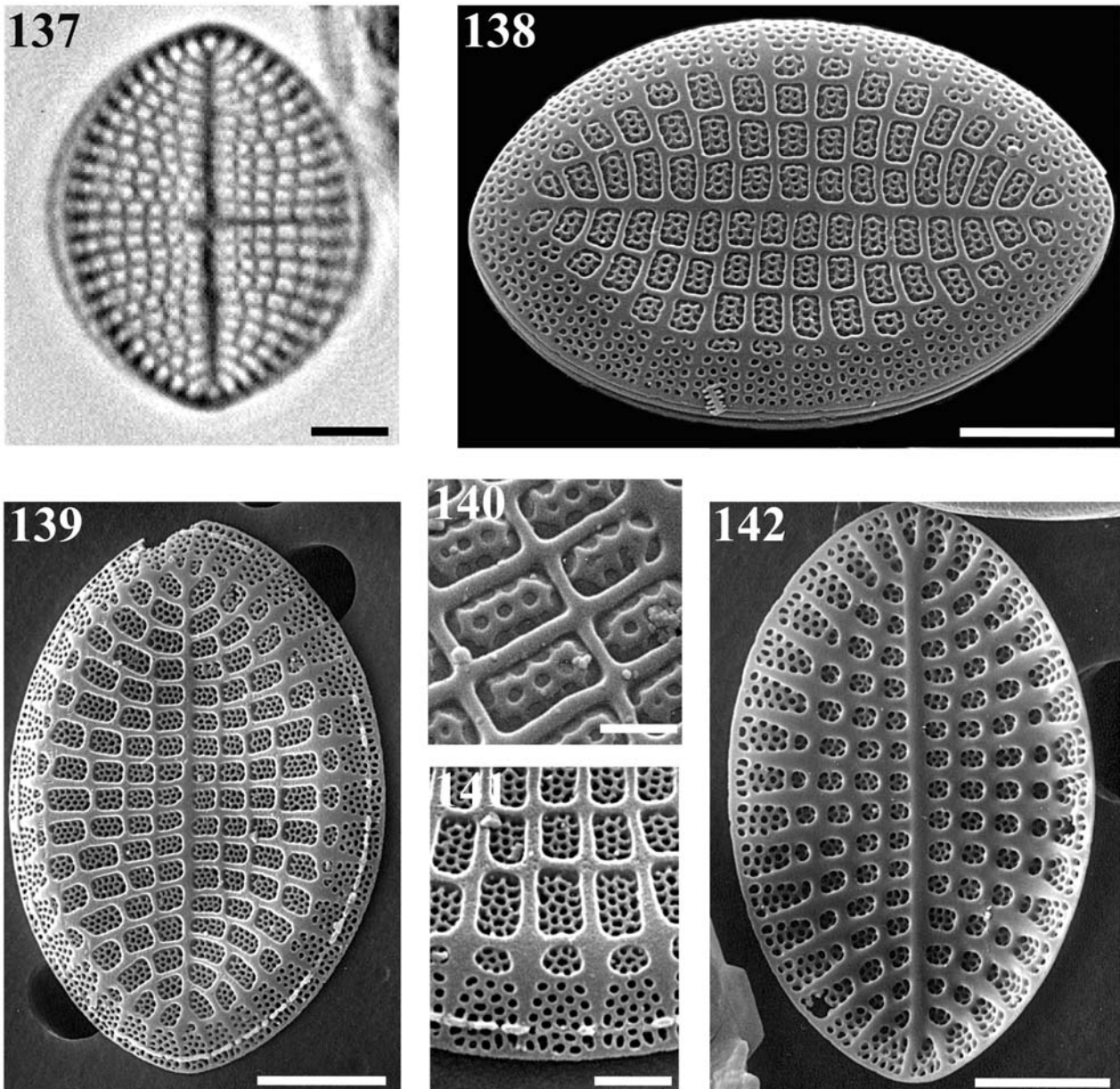
Possible synonyms *Cocconeis adjuncta* Schmidt 1894 in Schmidt et al. 1874–1959, pl. 190, figs. 15, 16



Figures 128–136 Sternum and raphe-sternum valves of *Cocconeis scutellum* var. *posidoniae* f. *decussata*.

(128) External view of the sternum valve. (129) Internal view of the sternum valve. (130) Internal view of the sternum valve showing the fimbriate and closed valvocopula. (131) Internal view of the sternum valve at 60° tilt. (132) Uniseriate striae of the sternum valve becoming bi- and triseriate on the mantle. Valve face poroid areolae are occluded by rotae with a single longitudinal bar. (133) Raphe-sternum valve in external view. (134) Raphe-sternum valve in internal view. (135) Internal distal raphe ending with helictoglossa on raphe-sternum valve. (136) Internal central raphe endings on raphe-sternum valve.

Figures 128–136, SEM. Scale bars=2 μm (Figures 128–134); 1 μm (Figures 135, 136).



Figures 137–142 Sternum valves of *Cocconeis scutellum* var. *sullivanensis*.

(137) Complete valve. (138) External valve view at 30° tilt. (139) Valve in external view. (140) Rectangular poroid areolae on the external valve face occluded by a complex volate cribrum consisting of three pores separated by silicified bars partially fused. (141) Poroid areolae with a series of small pores separated by a network of silicified bars. Tri- to pentaseriate poroid striae on the mantle. (142) Internal view of the valve.

Figure 137, LM; Figures 138–142, SEM. Scale bars=10 μm (Figures 137–139, 142); 1 μm (Figures 140, 141).

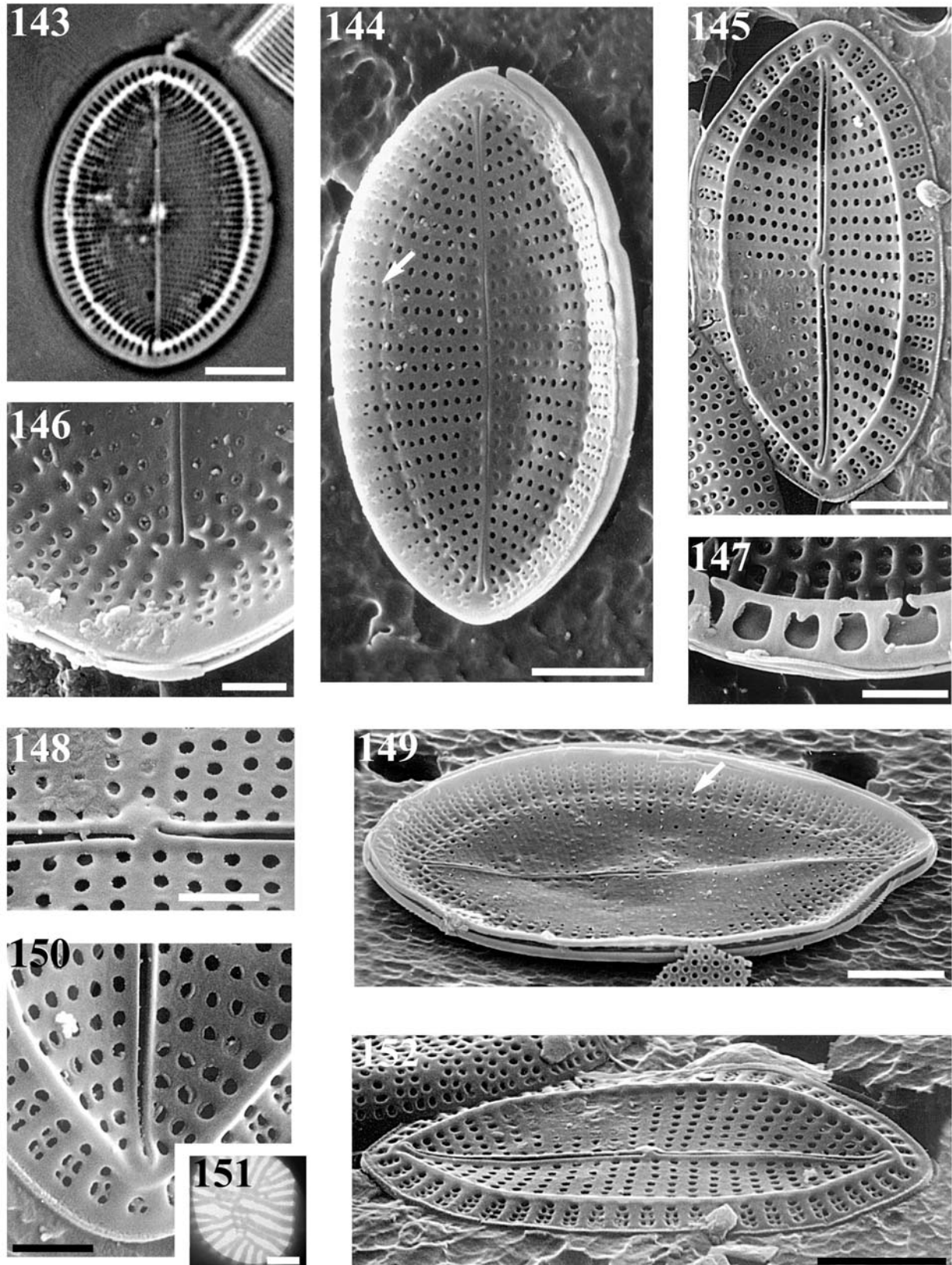
(Figure 2); *Cocconeis scutellum* var. *adjuncta* (Schmidt) Peragallo et Peragallo 1897–1908, p. 19, pl. 4, fig. 2 (Figure 3); *Cocconeis scutellum* var. *ampliata* Grunow 1880 in Van Heurck 1880–1885, pl. 29, figs. 4, 5.

Reference Cleve-Euler 1953, p. 7, fig. 489b.

LM and EM material Cleaned material from *Posidonia oceanica* leaves collected in the southern Tyrrhenian, Adriatic, and Aegean Seas, and slide E74 from the Hustedt Diatom Collection, Bremerhaven, Germany (Table 1).

Morphology The valve outline is elliptical to orbicular (Figures 36, 37, 44, 45). AA: 40–80 μm . TA: 30–60 μm .

Sternum valve (SV): In external view, the valve face is flat and the mantle slightly convex (Figure 43). The straight axial area lacks a central area and almost reaches the apex (Figures 36, 37). Striae, 7–9 in 10 μm , are uniseriate over most of the valve face (Figures 36, 37) and gradually becoming bi- to triseriate on the mantle (Figure 43). Interstriae are clearly visible and of a similar width (Figures 37, 43). The valve face is perforated by poroid areolae, 7–9 in 10 μm , arranged in an apically oriented pattern (Figures 37, 40, 41). The poroid areolae are thickened and quadrangular (Figure 38), and are internally occluded by a hymen with a central foramen (Figures 38, 39). The internal valve face has the same structure as the external face with, however, a stronger



Figures 143–152 Raphe-sternum valves of *Cocconeis scutellum* var. *sullivanensis*.

(143) Complete valve. (144) External view of the valve showing coaxial external proximal raphe endings. The submarginal hyaline area is only slightly visible (arrow). (145) Internal view of the valve. Note the submarginal hyaline area. (146) External terminal raphe ending. (147) Internal valve view showing the valvocopula. (148) Internal proximal raphe endings and central nodule. (149) External valve view at 60° tilt. Arrow indicates the inconspicuous submarginal hyaline area separating the valve face from the mantle. (150) Distal raphe ending with helictoglossa in internal view. (151) Poroid areola of the valve face showing the thin hymen with linear perforations of different length radially distributed on the margin. (152) Internal valve view at 60° tilt. Figure 143, LM; Figures 144–150, 152, SEM; Figure 151, TEM. Scale bars=10 μm (Figure 143); 5 μm (Figures 144, 145, 149, 152); 2 μm (Figures 146–148, 150); 0.1 μm (Figure 151).

Table 2 Morphometric data recorded for infraspecific taxa of *Cocconeis scutellum* from the literature and the present study.

Taxon	Reference	Apical axis (μm)	Transapical axis (μm)	SV striae in 10 μm	SV areolae in 10 μm	RSV striae in 10 μm	RSV areolae in 10 μm
<i>var. scutellum</i>	1	22–106	–	4.7–6.1	–	–	–
	5	45–60	11–30	8–10	–	8–10	–
	7	45–60	–	8	–	9–10	–
	14	20–60	12–40	5–8	5–8	7–9	10–12
	17	>50 >23	–	7–9 9.5–12	–	7.5–11 10.5–13.5	–
<i>var. scutellum f. birhaphidea</i>	19	22–46	11–35	10–12	14–16	10–13	16–18
<i>var. baldjickiana</i>	12	–	–	–	–	–	–
	8	32–46	18–22	–	–	–	–
	11	50	40	–	6	–	–
<i>var. bipunctata</i>	19	40–80	30–60	7–10	7–9	7–9	10–11
	6	57	36	4	–	–	–
<i>var. clinoraphis</i>	10	–	–	–	–	–	–
	19	25–45	22–36	7–8	6–8	8–11	10–12
<i>var. constricta</i>	10	24	14	–	–	–	–
<i>var. doljensis</i>	3	40–80	40–59	7 margin,	–	–	–
				12 center	–	–	–
<i>var. gorensis</i>	19	60–90	50–74	4	4–5	4	5–6
<i>var. inequalepunctata</i>	6	36–72	20–54	2–3	–	–	–
<i>var. japonica</i>	8	27	15	–	–	–	–
<i>var. minutissima</i>	2	8	6	17	–	–	–
	9	8	6	16	–	–	–
	14	10	–	17	–	–	–
<i>var. parva</i>	4	<30	–	11–14	–	–	–
	13	10–28	7–19	5–7	–	13–17	–
	16	9–17	5–11	9–13	–	9–14	10
	19	16–24	8–13	11	10	9–11	16
<i>var. posidoniae</i>	18	13–40	8–23	11–14	9–13	19–23	18–22
	19	16–36	12–24	12–14	10–12	18–23	19–22
<i>var. posidoniae f. decussata</i>	19	16–20	8–10	12–15	10–14	18–22	18–22
<i>var. pulchra</i>	6	72	60	3	–	–	–
<i>var. raeana</i>	4	48	36	10	5	–	–
<i>var. schmidtii</i>	9	12–24	10–24	8–10	–	12–14	8–10
<i>var. speciosa</i>	11	17–42	14–30	5–6	–	–	–
	15	24–26	20	–	–	–	–
	16	12–30	11–22	5–9	–	11–14	–
<i>var. sullivanensis</i>	19	30–56	20–46	4–6	3–4	14–16	20–22

1, Ehrenberg 1838; 2, Grunow in Van Heurck 1880–1885; 3, Pantocsek 1886–1903; 4, Cleve 1895; 5, Peragallo and Peragallo 1897–1908; 6, Missuna 1913; 7, Boyer 1927; 8, (Schmidt 1894; see Schmidt et al. 1874–1959) Skvortzow 1929; 9, Frenguelli 1930; 10, Zanon 1948; 11, Cleve-Euler 1953; 12, Jurilj 1957; 13, Okuno 1957; 14, Hustedt 1959; 15, Hendey 1964; 16, Poulin et al. 1984; 17, Mizuno 1987; 18, De Stefano et al. 2000; 19, present study.

RSV, raphe-sternum valve; SV, sternum valve.

silicification of the axial area and interstriae (Figures 40, 41). The valvocopula is closed and has digitate fimbriae expanded into lateral lobes (Figures 41, 42), or short fimbriae connected by siliceous flanges with sharp edges (Figure 52, arrows).

Raphe-sternum valve (RSV): Externally, the flat valve face is separated from a short and slightly concave mantle (Figures 45, 46) by a wide submarginal hyaline area (Figure 45). The raphe consists of two straight, thin fissures with drop-shaped proximal (Figure 50) and distal (Figure 46) external endings. The radiate, uniseriate valve face striae, 7–9 in 10 μm , (Figures 45, 51) are composed of circular poroids, 10–11 in 10 μm , occluded externally by hymenes with radially arranged perforations of different length (Figure 48). On the mantle they consist of a single poroid near the submarginal area followed by one or two rings of coupled poroids terminating far from the valve margin (Figures 45, 46, 47, 53). Internally, the submarginal hyaline area is thickened, slightly raised, and

bears apically elongated bumps at approximately every second interstria (Figures 52, 53). The internal raphe branches have proximal endings gently deflected in opposite directions, converging in a small, rounded and strongly silicified central nodule (Figure 49), and straight, slightly raised distal endings in small helictoglossae (Figure 47). The closed valvocopula has thin fimbriae extending over the thickened, submarginal rim of the valve (Figure 52). No observations are available on the ultrastructure of its *pars exterior*.

Taxonomic remarks Grunow (1888) described *Cocconeis scutellum var. baldjickiana*, but he subsequently raised it to species rank (Grunow 1894 in Schmidt et al. 1874–1959, pl. 190, figs. 7–10 [Figures 4, 5]). However, Cleve (1895) considered it as a variety of *C. scutellum*. Simultaneously, *C. adjuncta*, morphologically closely related to *C. scutellum var. baldjickiana*, was described by Schmidt (Schmidt et al. 1874–1959, pl. 190, figs. 15, 16

[Figure 2]), but later reassigned to the varietal status of *C. scutellum* by Peragallo and Peragallo (1897–1908, p. 19, pl. 4, fig. 2 [Figure 3]). However, both *C. scutellum* var. *baldjickiana* and var. *adjuncta* were rejected by Hustedt (1959) who considered them, together with *C. scutellum* var. *ampliata* Grunow in Van Heurck and var. *genuina* Cleve, as synonyms of the nominate variety, and he asserted the varieties “to be essentially as large well-developed individuals of the species, which [...] are bound to uninterrupted transitional forms and are almost always present simultaneously in the material”.

The biometric data for the valves were larger than those reported for the nominate variety (Table 2), and the shape of the poroid areolae on the SV was different. The areolae were sub-quadrangular in shape, with an external thickened margin and an internal hymen centrally pierced by a foramen (Figure 38). The irregular margins, sometimes expanded into lobes of the *pars interior* on the SV fimbriae are another characteristic feature of var. *baldjickiana* (Figures 41, 42). The poroid areolae on the RSV were smaller, and the numbers of striae and areolae (7–9 in 10 μm and 10–11 in 10 μm , respectively) were lower than in the nominate variety (Table 2). The mantle striae consisted of a single poroid close to the submarginal hyaline area and one or two rings of paired poroids (Figures 45, 47), which can also be observed in Grunow’s drawings (Schmidt et al. 1874–1959, pl. 190, figs. 7, 8 [Figure 4]).

Based on the previous structural valvar features differentiating them from the nominate variety, maintaining the varietal status of *Cocconeis scutellum* var. *baldjickiana* is appropriate. There is also a very strong resemblance between the illustrations of *C. adjuncta* – *C. scutellum* var. *adjuncta* in Schmidt et al. (1874–1959) and Peragallo and Peragallo (1897–1908) and *C. scutellum* var. *baldjickiana* (Figures 2, 3). Since we were unable to find the type material, we cannot provide further comparison between the structural valvar features of the two varieties. Therefore, we consider both *C. scutellum* var. *adjuncta* and var. *ampliata* as synonyms of *C. scutellum* var. *baldjickiana*.

Distribution *Cocconeis scutellum* var. *baldjickiana* was found in the Baltic Sea by Grunow (Schmidt et al. 1874–1959). We found specimens on *Posidonia oceanica* leaves at various locations in the Mediterranean Sea (Table 1), including a historical record from Lissa-Rovigno in Italy (slide E74, Friedrich-Hustedt Diatom Collection, Bremerhaven, Germany). The abundance of var. *baldjickiana* was always low in epiphytic communities, although high abundances of monospecific populations have been frequently recorded from the Adriatic Sea (De Stefano 2001).

***Cocconeis scutellum* var. *clinoraphis* Zanon (Figures 54–70)**

Basionym Zanon 1948, p. 211, fig. 15 (Figure 7).

LM and EM material Specimens scraped from *Posidonia sinuosa* leaves collected in Rottneest Island, Western Australia (Table 1).

Morphology The valve outline is elliptical to orbicular (Figures 54, 58, 64, 70). AA: 25–45 μm . TA: 22–36 μm .

Sternum valve (SV): Externally, the valve face ranges from flat to concave (Figure 55). The axial area is slightly sigmoid, never rectilinear and is interrupted before reaching the apex (Figures 54–58). Striae (7–8 in 10 μm) are uniseriate and radiate, becoming bi- to triseriate on the mantle (Figure 59). Each stria consists of large, circular poroids, 6–8 in 10 μm (Figures 59, 60), occluded by hymenes with linear perforations of different length, radially distributed at the margin. Internally, the striation resembles that of the external valve face (Figures 56, 57, 61). The valvocopula is closed (Figure 63) with long, digitate fimbriae (Figures 62, 63) reciprocally linked by siliceous flanges with sharp edges and connected to the valve at the interstriae (Figures 61, 62). Both advalvar and abvalvar surfaces of the valvocopula are smooth (Figures 61–63).

Raphe-sternum valve (RSV): The valve face is flat to concave (Figure 65) and clearly separated from the mantle by a submarginal hyaline area (Figure 64, arrow). The raphe is slightly sigmoid (Figures 64, 70) with the external proximal endings straight and reduced (Figures 64, 65), and the distal endings apically elongated (Figure 68). The striae, 8–11 in 10 μm , are uniseriate and radiate (Figures 64, 65, 70), and consist of circular poroid areolae, 10–12 in 10 μm , occluded by hymenes with linear perforations with a centric type array. On the mantle, the striae are bi- to triseriate consisting of smaller poroids (Figures 68, 69). The pattern on the internal valve resembles that on the external valve, except for the thickening of the raphe-sternum and the submarginal hyaline area (Figures 66, 67). The internal proximal raphe endings are almost coaxial (Figure 67), whereas the distal ones terminate in small helictoglossae close to the submarginal area (Figure 69). Valvocopula not observed.

Taxonomic remarks Based on examination of a single SV showing the presence of a slightly oblique sternum, Zanon (1948, p. 211, fig. 15 [Figure 7]) described *Cocconeis scutellum* var. *clinoraphis*. In our specimens, both the sternum and raphe-sternum are apically oriented, but slightly sigmoid. A certain degree of sigmoidicity can also be appreciated in Zanon’s original drawing (Figure 7). We have not been able to find Zanon’s original material, preventing further comparisons. Our specimens had a size range similar to that reported by Hustedt (1959) and Mizuno (1987) for the nominate variety.

Distribution So far, *Cocconeis scutellum* var. *clinoraphis* has been reported only from the type locality on the Sardinian coast in the Mediterranean basin (Zanon 1948). Our specimens have been reported in high abundances as epiphytes on Australian phanerogams (Table 1).

***Cocconeis scutellum* var. *gorensis* De Stefano var. nov. (Figures 71–89)**

Diagnosis *Valvae ellipticae-oblongae, 60–90 μm longae, 50–74 μm latae. Areovalva convexa in area axiali et in area marginali. Sternum lineare. Areovalvae habent structuram striis cum mono-seriatis (4 in 10 μm) quae constant ex areolis quadrangulis (4–5 in 10 μm) in fronte*

cellulae et in limbo oblongis. Areovalvae et raphovalvae frons cum linea longitudinali arcuata in utraque hemivalva. Raphovalva habet raphem rectam cum nodulo centrali elliptico. Striae (4 in 10 μm) constitutae sunt poroidis (5–6 in 10 μm) qui occlusi sunt hymenibus rimis cum inaequalibus. Areovalvae et raphovalvae valvocopula anuli forma clauditur. Utraque valvocopulae carent fimbriis internae faciei valvae tengens.

Valves elliptical to orbicular, 60–90 μm long, 50–74 μm large. Sternum valve convex in the axial area and toward the margin. The sternum is linear. The uniseriate striae of the SV (4–5 in 10 μm) consist of quadrangular areolae on the valve face and circular ones on the mantle. Sternum and raphe-sternum valve faces with longitudinal submarginal areas in each hemivalve. The RSV has a linear raphe and an elliptical central nodule. Striae (4 in 10 μm) consist of circular poroids (5–6 in 10 μm) occluded by hymenes with perforations of different lengths. Sternum and raphe-sternum valvocopulae are closed. Both valvocopulae have fimbriae extending over the internal valve faces.

Holotype Slide MDS 8 deposited at the Herbarium of the Stazione Zoologica of Naples, Italy.

Type locality Specimens scraped from *Posidonia coriacea* leaves in Nancy Cove, Philip Rock, Rottnest Island, Western Australia.

Etymology The name of this variety is dedicated to former U.S. vice-president, the honorable Mr. Al Gore, in recognition of his outstanding service in the promotion of public awareness of global change issues.

Morphology The valve outline is elliptical to orbicular (Figures 71, 80). AA: 60–90 μm . TA: 50–74 μm .

Sternum valve (SV): In external view, the valve face is flat to convex with a very wide mantle (Figures 71, 72). The axial area is linear and stops at some distance before reaching the valve margin by a submarginal area (Figure 74). The striae, approximately 4 in 10 μm , are uniseriate and parallel at the center, becoming radiate toward the apices (Figures 71, 74), and bi- to tetraseriate close to the margin (Figures 73, 74). The valve face striae consist of coarse sub-quadrangular poroids, 4–5 in 10 μm (Figures 73, 74, 76), which become circular and smaller on the valve-mantle area (Figure 73). Internally, the valve face has the same structure as the external surface, except for an expanded silicified submarginal area at the border between the valve face and mantle (Figure 75). The closed valvocopula has a narrow *pars exterior* and a *pars interior* consisting of thin fimbriae extending over the thickened submarginal area (Figure 77). Fimbriae have a central rib with thinner, laterally lobed extensions, which are fused with those of adjacent fimbriae creating an irregularly undulate distal margin in the valvocopula (Figures 78, 79, arrows) delimiting a series of large quadrangular openings (Figures 78, 79, asterisks). Both the abvalvar (Figure 78) and advalvar surfaces (Figure 79) of the *pars exterior* are smooth. Small thickenings in the margins of the fimbriae central ribs are evident in the advalvar surface (Figure 79, arrowhead).

Raphe-sternum valve (RSV): Externally, the valve face is flat to concave with a reduced mantle (Figures 80–82). The raphe is rectilinear (Figure 80) with proximal and distal endings straight and slightly apically expanded (Figures 83, 85). Striae (4 in 10 μm) are uniseriate and radial (Figures 80, 81), consisting of circular to apically elongate poroids, 5–6 in 10 μm (Figures 80, 83, 85). A submarginal hyaline area separates the uniseriate striation from the biseriate striae on the mantle (Figure 81, arrows), which consist of smaller subcircular poroids (Figures 82, 83). In some specimens, a row of small siliceous outgrowths is present near the valve's edge (Figure 83). The internal valve structure resembles the external one except for the thickened submarginal area, which has some apically elongate bumps (Figures 84, 86). The proximal raphe endings are slightly deflected in opposite directions (Figure 88), while the distal ones terminate in a small helictoglossa close to the submarginal area (Figures 86, 87). The valvocopula is closed, with digitate fimbriae at approximately every second interstria, and does not reach the submarginal area. The *pars exterior* of each fimbria bears an apically elongated papilla covered with horizontal furrows (Figure 89).

Taxonomic remarks The new variety *gorensis* differs from the nominate variety and the other varieties of *Cocconeis scutellum* by the high mean values of the transapical axis, the peculiar ultrastructure of SV and valvocopula, and the low values of stria density in both valves. The apical and transapical axes ranged from 60 to 90 μm and 50 to 74 μm , respectively (Table 2), which may contribute to the ovoid or orbicular shape of the valves. The number of striae and areolae (4 and 4–5/10 μm in SV; 4 and 5–6/10 μm in RSV, respectively) are less numerous than in the nominate and other varieties of *C. scutellum* (Table 2). Furthermore, the distinctive morphology of the SV is very peculiar with a reduced valve face and square poroid areolae bordered by a very wide mantle consisting of bi- to tetraseriate round poroid areolae. In addition, the delineation between the valve face and mantle is expanded internally in a strongly silicified submarginal hyaline area (Figure 75), which has never been observed in the SV of any other varieties of *C. scutellum*. The presence of a silicified submarginal hyaline area also explains the complex morphology of SV valvocopula fimbriae, which has lobed extensions (Figures 78, 79, arrows) reciprocally fused in a distal margin leaving an ovoid opening between two lobed extensions (Figures 78, 79, asterisks). As previously observed in the SV of *C. britannica* Nägeli in Kützing and *C. maxima* (Grunow) Peragallo et Peragallo, as well as in the RSV of almost all varieties of *C. scutellum*, the distal margin of the valvocopula fuses with the submarginal area, which acts as a supplementary valvar linking structure for the valvocopula (De Stefano et al. 2000). Papillae on the fimbriae of RSV valvocopulae are also peculiar, being distributed over almost all the entire surface of the fimbrial *pars interior*.

Distribution *Cocconeis scutellum* var. *gorensis* collected from Rottnest Island in Western Australia makes up a high proportion of the entire *Cocconeis* population

epiphytic on *Posidonia coriacea* leaves, but is less abundant on *Posidonia sinuosa*. This new variety was recently recorded from macroalgae collected on the coast of Siladen in Indonesia (C. Totti, personal communication).

***Cocconeis scutellum* var. *parva* (Grunow) Cleve (Figures 90–105)**

Basionym *Cocconeis scutellum* f. *parva* Grunow 1880 in Van Heurck 1880–1885, pl. 29, figs. 8, 9.

Synonyms *Cocconeis aggregata* Kützing 1844, p. 72, pl. 5, fig. VIII-5. *Cocconeis consociata* Kützing 1844, p. 72, pl. 5, fig. VIII-6. *Cocconeis transversalis* Gregory 1855, p. 39, pl. 4, fig. 7. *Cocconeis scutellum* var. *minor* Schmidt 1894 in Schmidt et al. 1874–1959, pl. 190, fig. 22.

References Peragallo and Peragallo 1897–1908, p. 20, pl. 4, fig. 3 (Figure 13); Hustedt 1930, p. 192, fig. 268; Okuno 1957, p. 221, pl. 7, fig. 1a–f; Hustedt 1959, p. 338, fig. 791; Gerloff and Helmcke 1977, fig. 954; Foged 1978, p. 42, pl. 14, fig. 11; John 1983, p. 82, pl. 36, figs. 5, 6; Noel 1984, p. 88, fig. 9; Poulin et al. 1984, p. 56, figs. 49–53; Riaux-Gobin 1991a, p. 129, pl. 2, figs. 9–11.

LM and EM material Cleaned material from *Posidonia oceanica* leaves collected in the western and eastern Mediterranean Sea (Table 1).

Morphology The valves are elliptical (Figures 90, 96). AA: 16–24 μm . TA: 8–13 μm .

Sternum valve (SV): In external view, the valve face is flat to convex, with a short mantle (Figure 91). The thin, straight axial area almost reaches the apex (Figures 90–92). Striae are radiate, 11 in 10 μm , uniseriate (Figures 90–92) and consist of large, circular poroid areolae, 10 in 10 μm , occluded by hymenes with linear perforations and irregularly distributed at the margin. Striae terminate on the mantle with apically elongated poroid areolae (Figures 92, arrow, 95). The width of interstriae, similar or larger than the striae, contributes to the apically aligned pattern of the poroid areolae (Figures 90, 92). Internally, the valve structure is similar to the external one except for the strongly silicified interstriae (Figures 92, 95). The valvocopula is closed (Figures 93, 94) with long digitate fimbriae (Figure 94).

Raphe-sternum valve (RSV): The external valve face is flat to concave with a reduced convex mantle (Figures 97, 105). The raphe is linear with slightly deflected (Figure 97) or straight (Figure 104) proximal endings (Figures 104, 105), and apically elongated and slightly expanded distal endings (Figures 100, 105). The uniseriate striae, 9–11 in 10 μm , are radiate (Figures 97, 105) and consist of small circular poroid areolae, 16 in 10 μm , occluded by hymenes (Figures 100, 104). On the mantle, each stria ends in a large, apically elongated poroid areola (Figure 98, arrow) close to the border between the valve face and mantle (Figure 97). Internally, the valve morphology reflects the external pattern except for the thickenings of the interstriae and raphe-sternum (Figure 99). The internal proximal raphe endings are slightly deflected in oppo-

site directions (Figure 102), while the distal endings terminate in small and raised helictoglossae (Figure 101). The valvocopula is closed and fimbriate (Figure 103). Fimbriae have an irregularly lobate *pars interior* and lack basal papillae (Figure 103).

Taxonomic remarks Originally described as *Cocconeis scutellum* f. *parva* by Grunow (Van Heurck 1880–1885), it was later elevated to a varietal status by Cleve (1895). The small size of the valves and the presence of large, apically elongated poroid areolae at the distal end of the striae in both SV and RSV easily distinguish var. *parva* from all other varieties of *C. scutellum* (Cleve 1895, Peragallo and Peragallo 1897–1908, Hustedt 1959, Archibald 1983). Poulin et al. (1984) suggested considering the regularity in the longitudinal pattern of the poroid areolae in the SV as an additional diagnostic feature of var. *parva*. Only few studies have recorded morphometric data for the RSV of var. *parva* (Okuno 1957, Poulin et al. 1984). The fine structure of the characteristic poroid areolae at the distal end of the striae has been studied by Okuno (1957) who pointed out the presence of complex volate hymenes “divided by net-veined partitions into about 7–10 micropores”.

The size ranges of our specimens (16–24 μm and 8–13 μm for SV and RSV, respectively) are within the range of those previously reported (Table 2). It is worth noting that in the RSV mantle, the apically elongated poroid areolae are not separated from the valve face striae by the presence of a submarginal area that is seen in other *C. scutellum* varieties. Their fine structure is similar to that reported by Okuno (1957).

There is some similarity between *Cocconeis scutellum* var. *parva* and var. *schmidtii* Frenguelli in the valve outline and morphometric data (Frenguelli 1930, p. 270, pl. 2, fig. 2 [Figure 16]), and also with var. *minutissima* Grunow (Van Heurck 1880–1885, pl. 29, fig. 12 [Figure 12]), although in the latter, the larger poroid areolae in the distal end of the striae are not evident (Cleve 1895).

Distribution Like the nominate variety, *Cocconeis scutellum* var. *parva* has a cosmopolitan distribution (Hustedt 1959, Gerloff and Helmcke 1977, Foged 1978, Archibald 1983, John 1983, Noel 1984, Poulin et al. 1984, Riaux-Gobin 1991a,b, Romero 1996, De Stefano 2001). In the Mediterranean Sea, its presence is documented for the Tyrrhenian Sea (Zanon 1948, Noel 1984, this study), Adriatic Sea (Cholnoky 1954), Aegean Sea (Foged 1986) and the Turkish coast (this study). This diminutive variety may colonize phanerogam leaves forming very dense, monospecific populations, especially in brackish and estuarine environments. In addition, it can also form epiphytic films on the larger conspecific varieties (e.g., *C. scutellum* var. *posidoniae*).

***Cocconeis scutellum* var. *posidoniae* De Stefano, Marino et Mazzella (Figures 106–127)**

Basionym De Stefano et al. 2000, p. 235, figs. 72–86.

References De Stefano 2001, p. 131, pl. 27, figs. 1–21; Sar et al. 2003, p. 83, figs. 10, 11.

LM and EM material Cleaned material from *Posidonia oceanica* leaves collected in the western and eastern Mediterranean Sea (Table 1).

Morphology The valve outline varies from broadly elliptical to elliptical-lanceolate (Figures 106, 107, 115, 116). AA: 16–36 μm . TA: 12–24 μm .

Sternum valve (SV): In external view, the valve face is convex and the mantle wide and smooth (Figures 107, 113). The linear axial area, which is slightly deepened in the valve face, lacks a central area (Figure 113) and terminates near the apex (Figures 107, 108). Striae are radiate (12–14 in 10 μm), uniseriate in the center of the valve face, biseriate at the margins and tri- to tetraseriate on the mantle (Figures 107, 108, 113). Interstriae are narrower than the striae, or of similar width (Figures 108, 112). The valve face is ornamented with poroid areolae, 10–12 in 10 μm , which are sub-quadrangular in shape in LM and internally occluded by rotate hymenes with two radial bars (Figures 108, 111). In large specimens, the rotae have a pierced, wide central area that is internally thickened (Figures 109, 110). Hymenes have linear perforations of different lengths, which are radially distributed on the margin (Figures 109, 111). The poroid areolae on the mantle are rounded, devoid of rotae and occluded by thin hymenes with centrally arranged perforations (Figure 108). The internal valve face has the same structure as the external one, with stronger silicified interstriae in both the valve face and the mantle, which also has sharp spines (Figures 112, 114). The closed valvocopula bears digitate fimbriae, which connect the interstriae at the valve margin (Figure 124).

Raphe-sternum valve (RSV): Externally, the valve face is flat or slightly concave on either side of the raphe (Figure 116) and is separated from the concave mantle by a submarginal hyaline area (Figures 115–117, arrow). The raphe is straight and thin with coaxial proximal endings (Figure 116), and distal endings terminating in reduced hyaline apical areas (Figures 116, 117). Striae, 18–23 in 10 μm , are radiate, uniseriate in the valve face up to the submarginal hyaline area and biseriate on the mantle (Figures 116–118). Striae consist of small circular poroid areolae, 19–22 in 10 μm , occluded externally by hymenes with radially arranged perforations of different length (Figure 118). Internally, the interstriae, raphe-sternum and submarginal areas are thickened (Figure 123). The submarginal hyaline area appears as an undulated rim with bumps and grooves corresponding to the striae and interstriae, respectively (Figure 120, arrows). Internally, the raphe possesses proximal endings slightly deflected in opposite directions converging to a rounded, strongly silicified central nodule (Figure 121), and distal endings terminating in reduced helictoglossae (Figure 122).

The closed valvocopula (Figures 124, 127) consists of a narrow *pars exterior* and a *pars interior* extending over the thickened, submarginal area of the valve (Figure 125) and consisting of fimbriae expanded in lateral lobes (Figure 126, arrows). The lobes of each fimbria fuse with adjacent ones generating a distal margin in the valvocopula (Figures 126, 127, arrows), which reduces the

interfimbrial spaces to large sub-quadrangular openings (Figures 126, 127, asterisks). On the abvalvar surface near the *pars exterior*, each fimbria bears a papilla covered by parallel transverse furrows (Figure 126, arrowhead).

Taxonomic remarks The variety *posidoniae* differs from the nominate variety in the stria density of both valves and the structure of the SV poroid areolae. The striae are more numerous with 11–14 in 10 μm and 19–23 in 10 μm in SV and RSV, respectively, than in the nominate variety and all other varieties of *Cocconeis scutellum*. The SV poroid areolae in var. *posidoniae* are sub-quadrangular in shape (Figures 108–111) and are externally occluded by rotate hymenes with two perpendicular bars (Figures 109, 111) (De Stefano et al. 2000). In large specimens, the rotae often have a central opening internally thickened (Figures 109, 110). Therefore, the SV poroid areolae of *C. scutellum* var. *scutellum* in TEM (Helmcke and Krieger 1953–1954, pls. 47, 48) must be attributable to var. *posidoniae* rather than var. *parva* as reported by Okuno (1957).

Five taxa of *Cocconeis scutellum*, namely var. *bipunctata* Missuna (Figure 6), var. *doljensis* Pantocsek (Figure 9), var. *inaequalepunctata* Missuna (Figure 10), var. *pulchra* Missuna (Figure 14) and var. *scutellum* f. *birhaphidea* Jurilj (Figure 18), were described based only on SV, and they all shared sub-rectangular poroid areolae and stria density varying between 4 and 9 in 10 μm (Pantocsek 1886–1903, Missuna 1913, Jurilj 1957). The differences among them mainly relied on the width of the sternum and the longitudinal arrangement of the poroid areolae. However, we consider the low number of SV poroid areolae in these five taxa as sufficient for rejecting their synonymy with *C. scutellum* var. *posidoniae*.

Cocconeis scutellum var. *speciosa* (Gregory) Cleve-Euler (Figure 17) is differentiated from all *C. scutellum* taxa by its small size range, sub-rhombic valve shape and squared areolae occluded by tetrapartite volae (Cleve-Euler 1953, Hustedt 1959, Hendeby 1964). This typical form of areolae makes var. *speciosa* closely related to var. *posidoniae*. In contrast, *C. scutellum* var. *constricta* (Figure 8), described by Zanon (1948) on the basis of SV characterized by a constriction at the valve center, should be rejected as a valid variety, because this constriction can be readily interpreted as a frustule deformation.

Distribution *Cocconeis scutellum* var. *posidoniae* is widespread in the Mediterranean Sea, where it is dominant in epiphytic diatom communities on phanerogams (De Stefano et al. 2000, De Stefano 2001). Okuno (1950) and Montgomery and Miller (1978) illustrated specimens of var. *posidoniae* collected in Awaji island and the Florida Keys, respectively but recorded them as *C. scutellum* var. *scutellum*. Sar et al. (2003) reported var. *posidoniae* in Argentinian coastal waters. Recent findings of *C. scutellum* var. *posidoniae* as an epiphyte on macroalgae and phanerogams from cold, temperate and tropical localities confirm it as a cosmopolitan variety (M. De Stefano, unpublished data).

***Cocconeis scutellum* var. *posidoniae* f. *decussata*
De Stefano f. nov. (Figures 128–136)**

Diagnosis *Valvae ellipticae, 16–20 μm longae, 8–10 μm latae. Areovalvae habent structuram striis cum mono-seriatis (12–15 in 10 μm) quae constant ex areolis quadrangulis (10–14 in 10 μm). Decussatae rotae partes exteriores areolarum occludunt.*

Valves elliptical, 16–20 μm long, 8–20 μm wide. Sternum valve with uniseriate striae (12–15 in 10 μm) consisting of quadrangular areolae (10–14 in 10 μm). Areolae externally occluded by rotae with a single longitudinal bar.

Holotype Slide MDS 9 deposited at the Herbarium of the Stazione Zoologica of Naples, Italy.

Type locality Otranto, southern Adriatic Sea, Italy.

LM and EM material Specimens collected from *Posidonia oceanica* leaves (Table 1).

Etymology The name of the form refers to the peculiar type of SV poroid occlusion: rotae with a single longitudinal bar.

Morphology The valves are elliptical (Figures 128, 129, 133, 134). AA: 16–20 μm. TA: 8–10 μm.

Sternum valve (SV): Externally, the valve face is convex and the mantle is wide and smooth (Figures 128, 129). The linear sternum lacks a central area (Figure 128) and terminates near the apex (Figures 128–131). The radiate striae (12–15 in 10 μm) are uniseriate in the center of the valve face, bi- or triseriate on the mantle (Figures 128, 129, 132). The valve face is ornamented with subquadrangular poroid areolae, 10–14 in 10 μm, internally occluded by rotate hymenes with a single longitudinal bar (Figure 132). Hymenes have linear perforations of different length, which are radially distributed on the margin. The mantle poroid areolae are rounded, devoid of rotae and occluded by thin hymenes with centrally arranged perforations. The internal valve face has the same structure as the external one, with more strongly silicified interstriae (Figure 131). The closed valvocopula bears digitate fimbriae, which connect the interstriae at the valve margin (Figure 130).

Raphe-sternum valve (RSV): The external valve face is flat to concave with a wide, convex mantle (Figure 133). The raphe is linear with straight proximal endings and apically elongated distal endings (Figure 133). The radiate striae, 18–22 in 10 μm (Figure 133), are uniseriate in the valve face up to the submarginal hyaline area and biseriate on the mantle (Figures 133–134), consisting of small circular poroid areolae, 18–22 in 10 μm, occluded by hymenes with centrally arranged perforations. Internally, the valve morphology reflects the external pattern, except for the thickenings of the raphe-sternum and the hyaline submarginal area (Figure 134). The internal proximal raphe endings are deflected in opposite directions (Figure 136), while the distal endings terminate in small and raised helictoglossae (Figure 135).

Taxonomic remarks The ultrastructural and morphometric features of our specimens resemble those of *Cocconeis scutellum* var. *posidoniae* (Table 2), except for the shape of the SV poroid hymenes and the higher number of RSV areolae (25–30 in 10 μm). In our specimens, areolae consist of rotae with a single longitudinal bar (Figures 128–132), whereas those of var. *posidoniae* have two perpendicular bars. The RSV ultrastructure is similar in both taxa (Figures 133–136).

Distribution *Cocconeis scutellum* var. *posidoniae* f. *decussata* has been only rarely recorded on *Posidonia oceanica* leaves, never forming monospecific populations, from the Adriatic Sea in Otranto, the type locality, and in Croatia and Slovenia (Table 1).

***Cocconeis scutellum* var. *sullivanensis* De Stefano var. nov. (Figures 137–152)**

Diagnosis *Valvae oblongae-ellipticae vel ellipticae, 30–56 μm longae, 20–46 μm latae. Areovalva leviter convexa in area marginali et complanata in area axiali. Areovalvae habent structuram striis cum mono-seriatis (4–6 in 10 μm) quae constant ex areolis rectangulis (3–4 in 10 μm) in fronte cellulae. Implicatae volae partes exteriores areolarum occludunt. In limbo cellulae, striae pluri-seriatae sunt et constant ex areolis oblongis cum implicatae volae et poroidis qui occlusi sunt hymenibus rimis cum inaequalibus.*

Valves orbicular-elliptical to elliptical, 30–56 μm long, 20–46 μm wide. Sternum valve slightly convex on the mantle and flat near the axial area. Sternum valve face with uniseriate striae (4–6 in 10 μm) consisting of rectangular areolae (3–4 in 10 μm). Multiseriate striae on mantle consisting of circular areolae occluded by complex volae or by hymenes with perforations of different length.

Holotype Slide MDS 10 deposited at the Herbarium of the Stazione Zoologica of Naples, Italy.

Type locality Forio, Ischia island, southern Tyrrhenian Sea, Italy.

LM and EM material Specimens collected from *Posidonia oceanica* leaves from Ischia Island, Italy (Table 1).

Etymology This variety is dedicated to Professor Michael Sullivan of the Florida State University in recognition for his outstanding contribution to epiphytic diatom research.

Morphology The valve outline varies from sub-rhomboid to elliptical-lanceolate (Figures 137–139, 142–144). AA: 30–56 μm. TA: 20–46 μm.

Sternum valve (SV): In external view, the valve face is convex and the mantle is wide (Figures 138, 139). The axial area is linear and terminates near the apex (Figures 137–139). Striae are radiate, 4–6 in 10 μm, uniseriate in the center of the valve face and the distal part of the mantle (Figures 138, 139), and becoming tri- to penta-

seriate on the remaining part of the mantle (Figure 141). The poroid areolae forming the striae, 3–4 in 10 μm , are rectangular in shape and are internally occluded by a complex volate cribrum consisting of three or more series of small pores separated by a network of silicified bars (Figure 141), sometimes partially fused (Figure 140). A single subcircular poroid areola occluded by a similar cribrum is present on the valve face-mantle border (Figure 141), whereas close to the valve margin, poroid areolae are smaller and occluded by hymenes with linear perforations of different length radially distributed. Interstriae are narrower than the striae and irregularly dispersed in the apical region (Figures 138, 139). The internal valve face has a similar structure to the external valve with, yet, stronger silicified interstriae (Figure 142). The valvocopula was not observed.

Raphe-sternum valve (RSV): The external valve face is concave on either side of the raphe (Figure 149). The raphe is straight and narrow, with coaxial proximal endings (Figure 144) and elongated distal endings terminating in reduced hyaline apical areas (Figure 146). The valve face is separated from the mantle by an inconspicuous submarginal hyaline area (Figures 144, 149, arrow). The radiate striae, 14–16 in 10 μm , are uniseriate on the valve face (Figure 144) and biseriate on the mantle (Figures 144, 146, 149). Striae consist of circular poroid areolae, 20–22 in 10 μm , occluded by external hymenes with radially arranged perforations of different length (Figure 151). Internally, the interstriae, raphe-sternum and submarginal area are thickened (Figures 145, 152). The submarginal area appears as an undulate rim exhibiting bumps and grooves corresponding to striae and interstriae, respectively (Figure 152). The internal proximal raphe endings are very slightly deflected in opposite directions and converge in a rounded silicified central nodule (Figure 148), while the distal endings terminate in small helictoglossae (Figure 150).

Taxonomic remarks The main diagnostic features of *var. sullivanensis* are the rectangular shape of SV poroid areolae and the internal volate cribrum consisting of three or more series of small pores separated by a network of silicified bars (Figures 138, 140). Striae and poroid areolae occur at very low density on the SV, similar to those reported for the new *var. gorenensis*, but densities on RSV resemble the values reported for *var. posidoniae*. Some specimens identified as *Cocconeis scutellum var. speciosa* by Poulin et al. (1984) had some morphometric measurements within the range of *var. sullivanensis*, but the former was clearly different in SV morphology and the characteristic squared poroid areolae.

Distribution *Cocconeis scutellum var. sullivanensis* has been recorded as an epiphyte on *Posidonia oceanica* meadows in a very restricted coastal area between Forio and Lacco Ameno in Ischia island. Specimens were also reported from Ventotene and Ponza islands, approximately 50 km from the type locality. Further observations are necessary to determine if this variety is endemic to Ischia and the Pontinian islands or whether it has a wider geographic distribution in the southern Tyrrhenian Sea and abroad.

Discussion

All varieties of *Cocconeis scutellum* share common morphological features in both sternum and raphe-sternum valves, but the architecture of the RSV is generally less variable than that of the SV. The shared valve features include: 1) elliptical to orbicular, monolayered valves, 2) narrow and mostly linear sternum and raphe-sternum, 3) uniseriate striae on the valve face changing in density and poroidal arrangement on the mantle, 4) submarginal hyaline area is usually present only on RSV, and 5) closed and always fimbriate valvocopulae, with papillate fimbriae on RSV. There are, however, other valvar characteristics differing among the varieties, such as 1) the shape and structure of the poroid areolae on SV, 2) the shape of fimbriae and papillae on the valvocopulae, and 3) the morphometric measurements. Our comparative study of these eight taxa of *C. scutellum* clearly indicates that these last three structural valvar characteristics allow for a reliable identification of the taxa.

Morphometric data alone do not allow for separation of taxa at the infraspecific level, since a continuum exists in the number of striae and poroid areolae of both valves among almost all varieties and forms of *Cocconeis scutellum* (Table 2). Therefore, we are proposing four distinct lineages among the varieties and forms of *C. scutellum* studied, relying mainly on the shape and structure of the poroid areolae on SV and the fimbriae on the valvocopula.

The first lineage is characterized by uniseriate striae on the valve face, with rounded or sub-quadrangular poroid areolae, which are occluded by simple hymenes consisting of linear perforations of different lengths, radially distributed on the margin; submarginal hyaline areas only present in RSV; digitiform SV and RSV fimbriae, but in the latter case with distal laterally expanded lobes and papillae. This lineage includes *Cocconeis scutellum var. scutellum*, *var. baldjikiana* and *var. clinoraphis*, the latter being the only one with slightly sigmoid sternum and raphe-sternum.

Taxa belonging to the second lineage share with the taxa of the first lineage the occurrence of uniseriate striae on the valve face, reduced bi- or triseriate striae on the mantle and submarginal hyaline areas only in RSV. However, they differ by having poroid areolae, which are occluded by rotate hymenes with one or two bars, volate hymenes or cribrum. This lineage includes *Cocconeis scutellum var. posidoniae* and *f. decussata*, and *var. sullivanensis*.

The third lineage is the only one characterized by wider striae on the SV mantle reaching nearly half of each hemivalve, a submarginal hyaline area also present on SV, a fimbriate valvocopula with fused distal lobes on SV and a digitate fimbriate valvocopula without lobes on RSV. It includes only *Cocconeis scutellum var. gorenensis*.

The last lineage includes *Cocconeis scutellum var. parva* which differs from all other varieties of *C. scutellum* by the absence of biseriate striae on the mantle, submarginal hyaline areas in both valves and papillae on RSV fimbriate valvocopula.

The valve structure illustrated by electron microscopy allowed us a complete characterization of *Cocconeis*

scutellum and most of its varieties. However, the question still remains as to where to draw the line between species and varieties within *C. scutellum*, particularly when differences between varieties seem to represent intraspecific morphological variability. A comparison of sequences of selected DNA regions of *C. scutellum* taxa would be very useful in addressing these questions.

Acknowledgements

The authors are indebted to Dr. R.M. Crawford and F. Hinz for their friendly cooperation and for having given the opportunity to observe types and samples from the Hustedt Diatom Collection in Bremerhaven, Germany. Thanks are also due to F.A.S. Sterrenburg, Dr. M. Poulin and both reviewers for constructive comments and nomenclatural and linguistic assistance with the final version of the manuscript.

References

- Anonymous. 1975. Proposal for a standardization of diatom terminology and diagnoses. *Nova Hedwigia, Beih.* 53: 323–354.
- Archibald, R.E.M. 1983. The diatoms of the Sundays and Great Fish rivers in the Eastern Cape Province of South Africa. *Bibl. Diatomol.* 1: 1–362.
- Boyer, C.S. 1927. Synopsis of the North American Diatomaceae. Part 2. *Proc. Acad. Nat. Sci. Phila., Suppl.* 79: 229–583.
- Cholnoky, B.J. 1954. Neue und seltene Diatomeen aus Afrika. *Österr. Bot. Z.* 101: 407–427.
- Cholnoky, B.J. 1963. Beiträge zur Kenntnis des marinen Littorals von Südafrika. *Bot. Mar.* 5: 38–83.
- Cleve, P.T. 1895. Synopsis of the naviculoid diatoms. Part II. *Kongl. Svenska Vetenskaps-Akad. Handl., Fjärde Ser.* 27: 1–235.
- Cleve-Euler, A. 1953. Die Diatomeen von Schweden und Finnland, Teil III. *Kongl. Svenska Vetenskaps-Akad. Handl., Fjärde Ser.* 4: 1–255.
- De Stefano, M. 2001. *Il genere Cocconeis (Bacillariophyta) nella comunità epifittica a diatomee di Posidonia oceanica: analisi tassonomica, ultrastrutturale ed ecologica*. Ph.D. thesis, University of Messina, Italy. pp. 245.
- De Stefano, M. and D. Marino. 2003. Morphology and taxonomy of *Amphicocconeis* gen. nov. (Achnanthesales, Bacillariophyceae, Bacillariophyta) with considerations on its relationship with other related monoraphid diatom genera. *Eur. J. Phycol.* 38: 361–370.
- De Stefano, M. and L. De Stefano. 2005. Nanostructures in diatom frustules: functional morphology of valvocopulae in Cocconeidacean monoraphid taxa. *J. Nanosci. Nanotech.* 5: 1–10.
- De Stefano, M. and O.E. Romero. 2005. A survey of alveolate species of the diatom genus *Cocconeis* (Ehr.) with remarks on the new section *Alveolatae*. *Bibl. Diatomol.* 52: 1–133.
- De Stefano, M., D. Marino and L. Mazzella. 2000. Marine taxa of *Cocconeis* on leaves of *Posidonia oceanica*, including a new species and two new varieties. *Eur. J. Phycol.* 35: 225–242.
- Ehrenberg, C.G. 1837. *Die fossilen Infusorien und die lebendige Dammerde. Vorgetragen in der Akademie der Wissenschaften zu Berlin 1836 und 1837*. Königl. Preuß. Akademie der Wissenschaften zu Berlin. pp. 27.
- Ehrenberg, C.G. 1838. *Die Infusionsthierchen als vollkommene Organismen. Ein Blick in das tiefere organische Leben der Natur*. Leopold Voss, Leipzig. pp. i–xvii, 1–548, Taf. 1–64 (Atlas).
- Ehrenberg, C.G. 1841. Verbreitung und Einfluss des mikroskopischen Lebens in Süd- und Nord-Amerika. 1. Berlin 1841. *In: Bericht über die zur Bekanntmachung geeigneten Verhandlungen der Königl. Preuß. Akademie der Wissenschaften zu Berlin*. Berlin. pp. 139–144, 202–209.
- Foged, N. 1975. Some littoral diatoms from the coast of Tanzania. *Bibl. Phycol.* 16: 1–127.
- Foged, N. 1978. Diatoms in Eastern Australia. *Bibl. Phycol.* 41: 1–243.
- Foged, N. 1984. Freshwater and littoral diatoms from Cuba. *Bibl. Diatomol.* 5: 1–248.
- Foged, N. 1986. Diatoms in Gambia, diatoms in the Volo Bay, Greece. *Bibl. Diatomol.* 12: 1–221.
- Foged, N. 1987. Diatoms from Viti Levu, Fiji Island. *Bibl. Diatomol.* 14: 1–194.
- Frenguelli, J. 1922–1924. Resultados de la primera Expedición a Tierra del Fuego (1921). Diatomeas de Tierra del Fuego. *An. Soc. Cient. Arg.* 96: 225–263.
- Frenguelli, J. 1930. Diatomeas marinas de la Costa Atlántica de Miramar. *An. Mus. Nac. Buenos Aires* 36: 243–312.
- Gaul, U., U. Geissler, M. Henderson, R. Mahoney and C.W. Reimer. 1993. Bibliography on the fine-structure of diatom frustule (Bacillariophyceae). *Proc. Acad. Nat. Sci. Phila.* 144: 69–238.
- Gerloff, J. and J.-G. Helmcke. 1977. *In: (J.-G. Helmcke and W. Krieger, eds.) Diatomeenschalen im elektronenmikroskopischen Bild*. Vol. 10. J. Cramer, Vaduz. pls. 924–1023.
- Giffen, M.H. 1980. A checklist of marine littoral diatoms from Mahé, Seychelles Islands. *Bacillaria* 3: 129–159.
- Gregory, W. 1855. On a post-tertiary lacustrine sand containing diatomaceous exuviae from Glenshira near Inverness. *Quart. J. Microsc. Sci.* 3: 30–43.
- Greuter, W., J. McNeill, F.R. Barrie, H.-M. Burdet, V. Demoulin, T.S. Filgueiras, D.H. Nicolson, P.C. Silva, J.E. Skog, P. Trehan, N.J. Turland and D.L. Hawksworth. 2000. *International code of botanical nomenclature (St Louis Code)*. Regnum Vegetabile 138. Koeltz, Königstein. pp. 1–474.
- Grunow, A. 1867–1870. Algae in “Reise der österreichischen Fregatte Novara um die Erde in den Jahren 1857, 1858, 1859”. *Bot. Theil.* 1: 1–104.
- Grunow, A. 1888. Referat über “Van Heurck, Henri. Types du synopsis des diatomées de Belgique. Ser. 5–22”. *Botanisches Centralblatt* 33: 323–325.
- Helmcke, J.G. and W. Krieger. 1953–1954. *Diatomeenschalen im elektronenmikroskopischen Bild*. Part II. Bild und Forschung, Berlin. pls. 103–200.
- Hendey, N.I. 1964. *An introductory account of the smaller algae of British coastal waters. Part V. Bacillariophyceae (diatoms)*. Her Majesty’s Stationary Office, London. pp. 317.
- Holmes, R.W., R.M. Crawford and F.E. Round. 1982. Variability in the structure of the genus *Cocconeis* Ehr. (Bacillariophyta) with special reference to the cingulum. *Phycologia* 21: 370–381.
- Hustedt, F. 1930. Bacillariophyta (Diatomeae). *In: (A. Pascher, ed.) Die Süßwasserflora Mitteleuropas*. G. Fischer, Jena. pp. 1–466.
- Hustedt, F. 1959. Die Kieselalgen Deutschlands, Österreichs und der Schweiz unter Berücksichtigung der übrigen Länder Europas sowie der angrenzenden Meeresgebiete. *In: (L. Rabenhorst, ed.) Kryptogamen-Flora von Deutschland, Österreich und der Schweiz*. Band 7, Teil 2. Akademische Verlagsgesellschaft, Leipzig. pp. 321–576.
- John, J. 1983. The diatom flora of the Swan River Estuary, Western Australia. *Bibl. Phycol.* 64: 1–359.
- Jurilj, A. 1957. Diatomije sarmatskog mora okoline Zagreba. (Flora of diatoms of Sarmatic Sea in environs of Zagreb). *Acta Biol.* 1: 1–154.
- Karsten, G. 1928. Bacillariophyta (Diatomaceae). *In: (A. Engler and K. Prantl, eds.) Die natürlichen Pflanzenfamilien. Band 2: Peridinea, (Dinoflagellatae), Diatomeae (Bacillariophyta), Myxomycetes*. 2. Auflage. Wilhelm Engelmann, Leipzig. pp. 105–303.

- Kobayasi, H. and T. Nagumo. 1985. Observations on the valve structure of marine species of the diatom genus *Cocconeis* Ehr. *Hydrobiol.* 127: 97–103.
- Kützing, F.T. 1844. *Die kieselschaligen Bacillarien oder Diatomeen*. Nordhausen. pp. 152.
- Lange-Bertalot, H. and K. Krammer. 1989. *Achnanthes, eine Monographie der Gattung, mit Definitionen der Gattung Cocconeis und Nachträgen zu den Naviculaceae*. J. Cramer, Berlin/Stuttgart. pp. 393.
- Mann, D.G. 1981. Sieves and flaps: siliceous minutiae in the pores of raphid diatoms. In: (R. Ross, ed.) *Proceedings of the 6th Symposium on recent and fossil diatoms*. Koeltz, Königstein. pp. 279–295.
- Mazzella, L., M.C. Buia and L. Spinoccia. 1994. Biodiversity of an epiphytic diatom community on leaves of *Posidonia oceanica*. In: (D. Marino and M. Montresor, eds.) *Proceedings of the 13th International diatom symposium*. Biopress, Bristol. pp. 241–251.
- Missuna, A. 1913. *Beiträge zur Kenntniss der fossilen Diatomeen Südrusslands*. Collection of papers commemorating the 25th anniversary of Prof. V.I. Vernadsky. Vol. 1. pp. 138–175.
- Mizuno, M. 1987. Morphological variation of the attached diatom *Cocconeis scutellum* var. *scutellum* (Bacillariophyceae). *J. Phycol.* 23: 591–597.
- Montgomery, R.T. and W. Miller. 1978. *Environmental and ecological studies of the diatom communities associated with the coral reefs of the Florida Keys. Vol. II. A taxonomic study of Florida Keys: benthic diatoms based on SEM*. Ph.D. thesis, Florida State University, College of Art and Sciences, Florida. pp. 541.
- Navarro, J.N. 1982a. Marine diatoms associated with mangrove prop roots in the Indian River, Florida, USA. *Bibl. Phycol.* 61: 1–151.
- Navarro, J.N. 1982b. A survey of the marine diatoms of Puerto Rico. V. Suborder Raphidineae: families Achnantheaceae and Naviculaceae (excluding *Navicula* and *Mastogloia*). *Bot. Mar.* 25: 321–338.
- Noel, D. 1984. Les diatomées des saumures et des sédiments de surface du Salin de Bras del Port (Santa Pola, Province d'Alicante, Espagne). *Rev. Inv. Geol.* 38/39: 79–107.
- Ognjanova-Rumenova, N. and E.P. Zapryanova. 1998. Siliceous microfossil stratigraphy of sediment profile "F" connected with archaeological excavation in coastal wetlands in the Bay of Sozopol (Bulgarian Black Sea coast). *Phytol. Balcan.* 4: 65–80.
- Okuno, H. 1950. Electron-microscopical study of the fine structure of diatom frustules. VIII. *Bot. Mag.* 63: 97–106.
- Okuno, H. 1957. Electron-microscopical study of the fine structure of diatom frustules. XVI. *Bot. Mag.* 70: 216–222.
- Pantocsek, J. 1886–1903. *Beiträge zur Kenntnis der fossilen Bacillarien Ungarns. Teil I: Marine Bacillarien*. W. Junk, Berlin. pp. 74.
- Peragallo, H. and M. Peragallo. 1897–1908. *Diatomées marines de France et des districts maritimes voisins*. M.J. Tempère, Grez-sur-Loing. pp. 492.
- Poulin, M., L. Bérard-Therriault and A. Cardinal. 1984. Les diatomées benthiques de substrats durs des eaux marines et saumâtres du Québec. 1. Cocconeioideae (Achnanthes, Achnantheaceae). *Nat. Can.* 111: 45–61.
- Rabenhorst, L. 1853. *Die Süßwasser-Diatomeen (Bacillarien) für Freunde der Mikroskopie*. Edward Kummer, Leipzig. pp. 72.
- Rabenhorst, L. 1864. *Flora europaea algarum aquae dulcis et submarinae. Sectio I. Algas diatomaceas complectens, cum figuris generum omnium xilographice impressis*. Apud Eduardum Kummerum, Lipsiae. pp. 359.
- Riaux-Gobin, C. 1991a. Diatomées d'une vasière intertidale du Nord Finistère (Dourduff): genres *Cocconeis*, *Campyloneis*, *Delphineis*, *Mastogloia* et *Rhaphoneis*. *Diatom Res.* 6: 125–135.
- Riaux-Gobin, C. 1991b. The diatom genus *Cocconeis* from an intertidal mud flat of North Brittany: source and diversity. *Can. J. Bot.* 69: 597–601.
- Riaux-Gobin, C. and H. Germain. 1980. Peuplement de diatomées épipéliques d'une slikke de Bretagne Nord. Importance relative du genre *Cocconeis* Ehr. *Cryptogam. Algol.* 1: 265–279.
- Riaux-Gobin, C. and O.E. Romero. 2003. Marine *Cocconeis* Ehrenberg (Bacillariophyceae) species, and related taxa, from Kerguelen's Land (Austral Ocean, Indian Sector). *Bibl. Diatomol.* 47: 1–189.
- Ricard, M. 1977. Les peuplements de diatomées des lagons de l'archipel de la Société (Polynésie Française): floristique, écologie, structure de peuplements et contribution à la production primaire. *Rev. Algol.* 12: 137–336.
- Rivera, P. 1983. A guide for references and distribution for the class Bacillariophyceae in Chile between 18°28'S and 58°S. *Bibl. Diatomol.* 3: 1–386.
- Rivera, P., O. Parra and M. Gonzalez. 1973. Fitoplancton del Estero Lenga, Chile. *Gayana Bot.* 23: 1–93.
- Romagnoli, T., G. Bavestrello, E.M. Cucchiari, M. De Stefano, C.G. Di Camillo, C. Pennesi, S. Puce and C. Totti. 2006. Microalgal communities epibiotic on the marine hydroid *Eudendrium racemosum* in the Ligurian Sea during an annual cycle. *Mar. Biol.* 151: 537–552.
- Romero, O.E. 1996. Ultrastructure of four species of the diatom genus *Cocconeis* Ehr. with the description of *C. pseudocostata* sp. nov. *Nova Hedwigia* 63: 361–396.
- Romero, O.E. and J.N. Navarro. 1999. Two marine species of *Cocconeis* Ehrenberg (Bacillariophyceae): *C. pseudomarginata* Gregory and *C. caribensis* sp. nov. *Bot. Mar.* 42: 581–592.
- Ross, R., E.J. Cox, N.I. Karayeva, D.G. Mann, T.B.B. Paddock, R. Simonsen and P. Sims. 1979. An amended terminology for the siliceous components of the diatom cell. *Nova Hedwigia, Beih.* 64: 513–533.
- Round, F.E., R.M. Crawford and D.G. Mann. 1990. *The diatoms. Biology and morphology of the genera*. Cambridge University Press, Cambridge. pp. 747.
- Sar, A., O. Romero and I. Sunesen. 2003. *Cocconeis* Ehrenberg and *Psammococconeis* Garcia (Bacillariophyta) from the Gulf of San Matias, Patagonia, Argentina. *Diatom Res.* 18: 79–106.
- Schmidt, A., M. Schmidt, F. Fricke, H. Heiden, O. Müller and F. Hustedt. 1874–1959. *Atlas der Diatomaceen-Kunde*. 4 volumes. O.R. Reissland, Leipzig. pls. 480.
- Skvortzow, B.W. 1929. Marine diatoms from Dairen, South Manchuria. *Philipp. J. Sci.* 38: 419–427.
- Smith, W. 1853–1856. *Synopsis of British Diatomaceae*. Vol. 1. John Van Voorst, London. pp. 89.
- Sullivan, M.J. 1979. Epiphytic diatoms of three seagrass species in Mississippi Sound. *Bull. Mar. Sci.* 29: 459–464.
- Sullivan, M.J. 1981. Community structure of diatoms epiphytic on mangroves and *Thalassia* in Bimini Harbour, Bahamas. In: (R. Ross, ed.) *Proceedings of the 6th Symposium on recent and fossil diatoms*. Koeltz, Königstein. pp. 385–398.
- Sullivan, M.J. 1982. Community structure of the epiphytic diatoms from the Gulf Coast of Florida, U.S.A. In: (D.G. Mann, ed.) *Proceedings of the 7th International diatom symposium*. Koeltz, Königstein. pp. 373–384.
- Totti, C., E. Cucchiari, M. De Stefano, C. Pennesi, T. Romagnoli and G. Bavestrello. 2007. Seasonal variations of epilithic diatoms on different hard substrata, in the northern Adriatic Sea. *J. Mar. Biol. Ass. UK* 87: 649–658.
- Van Heurck, H. 1880–1885. *Synopsis des diatomées de Belgique*. H. Van Heurck, Anvers. pp. 235, pls. 135.
- Van Heurck, H. 1896. *Traité des diatomées*. H. Van Heurck, Anvers. pp. 558, pls. 35.
- VanLandingham, S.L. 1968. *Catalogue of the fossil and recent genera and species of diatoms and their synonyms. Part II. Bacteriastrum through Coscinodiscus*. J. Cramer, Vaduz. pp. 494–1086.

- VanLandingham, S.L. 1979. *Catalogue of the fossil and recent genera and species of diatoms and their synonyms. Part VIII. Supplementary taxa (through 1964). Supplementary references. Synonymy addendum. Correction. Additions.* J. Cramer, Vaduz. pp. 4242–4654.
- Witkowski, A., H. Lange-Bertalot and D. Metzeltin. 2000. Diatom flora of marine coasts I. *Iconogr. Diatomol.* 7: 1–907.
- Wolle, F. 1890. *Diatomaceae of North America, illustrated with twenty-three hundred figures from the author's drawings on one hundred and twelve plates.* Comenius Press, Bethlehem, USA. pls. 112.
- Zanon, D.V. 1948. Diatomee marine di Sardegna e puggilo di alghe marine della stessa. *Acta Pontif. Acad. Sci.* 12: 202–246.

Received 3 September, 2007; accepted 22 September, 2008